

# A Two-Stage Bayesian Approach for Variable Selection in Joint Modeling of Multiple Longitudinal Markers with Competing Risks

Taban Baghfalaki<sup>1,2\*</sup>, Reza Hashemi<sup>3</sup>, Christophe Tzourio<sup>2</sup>,  
Catherine Helmer<sup>2</sup>, Helene Jacqmin-Gadda<sup>2</sup>

<sup>1</sup>Department of Mathematics, The University of Manchester,  
Manchester, UK.

<sup>2</sup>Inserm, Research Center U1219, Univ. Bordeaux, ISPED, F33076  
Bordeaux, France.

<sup>3</sup>Department of Statistics, Razi University, Kermanshah, Iran.

\*Corresponding author(s). E-mail(s):  
[taban.baghfalaki@manchester.ac.uk](mailto:taban.baghfalaki@manchester.ac.uk);

## Abstract

In many clinical and epidemiological studies, collecting both longitudinal measurements and time-to-event outcomes is essential. Accurately estimating the relationships between longitudinal markers and time-to-event outcomes, as well as identifying key longitudinal markers for risk prediction, is critical, especially in the presence of competing risks, where multiple types of events can occur. However, as the number of longitudinal markers increases, fitting joint models becomes increasingly challenging, often resulting in long computation times or convergence issues. In this paper, we propose a novel two-stage Bayesian approach for variable selection in joint models that accommodate multiple longitudinal markers and competing risks outcomes. Our method is designed to efficiently identify significant longitudinal markers and covariates. In the first stage, we fit a one-marker joint model for each longitudinal marker together with the competing risks event. These estimates are then used to predict individual marker trajectories, mitigating bias caused by informative dropout. In the second stage, we fit a cause-specific hazards model for competing risks, incorporating the predicted current values of all markers as time-dependent covariates. We explore both continuous and Dirac spike-and-slab priors for variable selection within a Bayesian

framework, using Markov chain Monte Carlo (MCMC) techniques. Our approach enables risk prediction based on a large number of longitudinal markers—a task that is often considered infeasible in standard joint modeling approaches. We rigorously evaluate our method through simulation studies, assessing both parameter estimation and predictive performance. Finally, we illustrate the practical utility of our approach by predicting the risk of dementia using the Three-City (3C) dataset, a longitudinal cohort study conducted in France, where competing risks of death are present. To facilitate implementation, we provide an R package, `VSJM`, freely available at <https://github.com/tbaghfalaki/VSJM>.

**Keywords:** Joint modeling, Variable selection, Markov chain Monte Carlo (MCMC), Sparsity, Spike and slab priors.

## 1 Introduction

In many clinical studies, longitudinal measurements are repeatedly collected for each subject at different time points until an event such as death or drop-out occurs. It is also common to have multiple longitudinal measurements in a study. For example, in the context of HIV/AIDS studies, two important markers that are often repeatedly measured until death or drop-out are HIV-RNA and CD4 [1]. In most of these types of studies, the number of longitudinal markers under investigation and the number of explanatory variables is large. Estimating the association between longitudinal markers and time-to-event outcomes, as well as determining the effect of explanatory variables on event risks, is crucial in modern medicine [2–6], in particular, for the development of individual risk prediction models [7, 8]. For this purpose, joint models for longitudinal and time-to-event outcomes that combine mixed models and time-to-event models, have received considerable attention over the past decades. Interesting reviews on joint modeling can be found in [9–11] and [12]. From a computational point of view, the R software now offers some options: `JMbayes` [13], `JMbayes2` [14], `INLAjoint` [15], and `stan_jm` modelling function in the `rstanarm` package [16]. The Bayesian implementation of joint models with multiple markers is available through `INLAjoint` [15] and `JMbayes2` [14], but dealing with a large number of markers still poses computational difficulties due to the large number of random effects and parameters in these models. For this purpose, [17] propose a novel two-stage joint modeling approach (TSJM). In the first stage, separate joint models are fitted for each biomarker and the time-to-event outcome. In the second stage, the predicted linear predictors from each biomarker-specific model are incorporated as time-dependent covariates in a semi-parametric Cox model. This strategy improves computational tractability and mitigates bias arising from informative dropout. In their study, [17] compared the TSJM with the standard two-stage (STS) approach and a multi-marker joint model (MMJM), evaluating performance in terms of parameter estimation and dynamic prediction. Their results indicate that when the number of biomarkers is small, TSJM performs comparably to MMJM, while the STS approach performs poorly, particularly when the biomarkers are strongly correlated. Furthermore, when the number of

biomarkers is large, MMJM exhibits limited estimation reliability, whereas TSJM provides a more favorable balance between estimation accuracy and model stability.

When multiple longitudinal markers and large number of time-invariant explanatory variables, are considered, the selection of the most predictive variables is challenging. Traditionally this has been performed through model comparison criteria such as Akaike Information Criterion (AIC), Bayesian Information Criterion (BIC), or Deviance Information Criterion (DIC). The use of these criteria for complex models in the presence of a large number of candidate models is not feasible due to the computational complexity associated with evaluating these criteria for complex models with numerous parameters and candidate models. Consequently, traditional criteria may not effectively guide model selection in such complex scenarios. This has led to the exploration of alternative strategies, such as variable selection, to address these challenges and identify the most appropriate model. It involves choosing appropriate variables from a complete list and removing those that are irrelevant or redundant. The purpose of such selection is to determine a set of variables that will provide the best fit for the model in order to make accurate predictions [18]. In general, variable selection in the frequentist paradigm involves the utilization of a penalized likelihood approach, which considers various forms of penalty functions. These include the least absolute shrinkage and selection operator (LASSO), the smoothly clipped absolute deviation (SCAD), and the adaptive least absolute shrinkage and selection operator (ALASSO) [19]. In the Bayesian framework, the selection of appropriate priors plays a pivotal role, similar to the regularization and shrinking techniques employed in frequentist variable selection methods. Properly chosen priors not only inform the prior beliefs about model parameters but also contribute to the regularization of the model, aiding in the prevention of overfitting and the promotion of model parsimony [20]. In this paper, we delve into the realm of Bayesian variable selection, where the careful selection of priors allows for the automatic identification of relevant predictors while appropriately handling model complexity [21]. Various types of priors have been proposed for variable selection, including spike-and-slab priors [21–23], horseshoe prior [24], and Laplace (i.e., double-exponential) prior [25]. Our investigation focuses on two prominent types of priors: continuous and Dirac spike priors. These priors strike a balance between flexibility and simplicity, offering practical advantages in the context of variable selection [26]. By exploring the implications and effectiveness of these priors, we aim to provide insights into their utility and contribute to the ongoing discourse surrounding Bayesian variable selection methodologies.

Variable selection methods in joint modeling have been explored across various studies, each offering unique insights into different aspects of the modeling process. [27] employed a penalized likelihood approach with adaptive LASSO penalty functions to select fixed and random effects in joint modeling of one longitudinal marker and time-to-event data. [28] extended this approach to the joint analysis of longitudinal data and interval-censored failure time data, utilizing penalized likelihood-based procedures to simultaneously select variables and estimate covariate effects. [29] adopted gradient boosting for variable selection in joint modeling, providing an alternative method for addressing this task. [30] utilized L1 penalty functions to select random effects and off-diagonal elements in the covariance matrix in the survival sub-model. Their focus was

on joint modeling of multiple longitudinal markers and time-to-event data within the frequentist paradigm. [31] considered simultaneous parameter estimation and variable selection in joint modeling of longitudinal and survival data using various penalized functions. [32] utilized a B-spline decomposition and penalized likelihood with adaptive group LASSO to select the relevant independent variables and distinguish between the time-varying and time-invariant effects for the two sub-models. On the Bayesian side, [33] proposed a semiparametric joint model for analyzing multivariate longitudinal and survival data. They introduced a Bayesian Lasso method with independent Laplace priors for parameter estimation and variable selection. However, these studies primarily focused on scenarios with a limited number of longitudinal markers and did not address cases where the number of markers is high. Additionally, dynamic prediction in the context of variable selection in joint modeling remains unexplored in the literature reviewed here.

In this paper, we consider variable selection, including the selection of both the longitudinal markers and the time-invariant covariates, in the joint modeling of multiple longitudinal measurements and competing risks outcomes. This is the first study to specifically address variable selection in this context. For this purpose, we are faced with two issues. The first challenge is estimating joint models including a large number of longitudinal markers, which may be unfeasible. The second challenge, which involves variable selection, is addressed by using a spike-and-slab prior in a Bayesian paradigm. As a summary, we propose a new two-stage approach for variable selection of multiple longitudinal markers and competing risks outcomes when the number of longitudinal markers and covariates is large, and the estimation of the full joint model including all the markers and covariates is intractable. Using a Bayesian approach, the first stage involves estimating one-marker joint models for the competing risks and each longitudinal marker as in [17]. This avoids the bias caused by informative dropout. In the second stage, extending TSJM, we estimate a cause-specific hazard model for the competing risks outcome using a Bayesian approach allowing variable selection using a Bayesian approach allowing variable selection. This model includes time-dependent covariates and incorporates spike-and-slab priors. The explanatory variables in the hazard model consist of the estimates of functions derived from the random effects and parameters obtained from the initial stage of jointly modeling each longitudinal marker. We provide an R-package `VSJM` that implements the proposed methods which is available at <https://github.com/tbaghfalaki/VSJM>.

This paper is organized as follows: In Section 2, we describe our variable selection approach, which includes introducing longitudinal and competing risks sub-models, reviewing parameter estimation in MMJM, and finally describing our proposed two-stage approach for Bayesian variable selection. Section 3 focuses on dynamic prediction using the proposed approach. Section 4 presents a simulation study comparing the behavior of the variable selection two-stage approach with the oracle joint model in terms of variable selection and dynamic prediction. In Section 5, the proposed approach is applied to variable selection and the risk prediction of dementia in the Three-City (3C) cohort study [34]. Finally, the last section of the paper includes a conclusion of the proposed approach.

## 2 Variable selection for joint modeling

The observed time for subject  $i$  is defined as  $T_i = \min(T_{i1}^*, \dots, T_{iL}^*, C_i)$ , where  $T_{il}^*$  denotes the time to event  $l$  and  $C_i$  is the censoring time. The corresponding event indicator is denoted by  $\delta_i \in \{0, 1, \dots, L\}$ , where  $\delta_i = 0$  indicates censoring and  $\delta_i = l$  indicates the occurrence of event  $l$ . We assume that the censoring times  $C_i$  are independent of the event times  $(T_{i1}^*, \dots, T_{iL}^*)$ , i.e., censoring is non-informative. Let  $Y_{ijk} = Y_{ik}(s_{ijk})$  denote the value of the  $k$ th longitudinal marker for subject  $i$  at time  $s_{ijk}$ . As a result, consider  $\{T_i, \delta_i, Y_{ijk} \mid i = 1, \dots, N; j = 1, \dots, n_i; k = 1, \dots, K\}$  as a sample from the target population, where  $i$  indexes the subjects in the study,  $j$  indexes the repeated measurements for subject  $i$  with  $n_i$  denoting the total number of longitudinal measurements observed for subject  $i$ , and  $k$  indexes the different longitudinal markers.

### 2.1 Longitudinal sub-model

A multivariate linear mixed-effects model is considered for the multiple longitudinal markers as follows:

$$Y_{ijk} = \eta_{ik}(s_{ijk} | \boldsymbol{\beta}_k, \mathbf{b}_{ik}) + \varepsilon_{ijk}, i = 1, \dots, N, j = 1, \dots, n_i, k = 1, \dots, K, \quad (1)$$

where  $\varepsilon_{ijk} \stackrel{\text{iid}}{\sim} N(0, \sigma_k^2)$ . We assume that

$$\eta_{ik}(s | \boldsymbol{\beta}_k, \mathbf{b}_{ik}) = \mathbf{X}_{ik}(s)^\top \boldsymbol{\beta}_k + \mathbf{Z}_{ik}(s)^\top \mathbf{b}_{ik}, k = 1, \dots, K, \quad (2)$$

where  $\mathbf{X}_{ik}(s)$  and  $\mathbf{Z}_{ik}(s)$  are the design vectors at time  $s$  for the  $p_k^\beta$ -dimensional fixed effects  $\boldsymbol{\beta}_k$  and  $q_k$ -dimensional random effects  $\mathbf{b}_{ik}$ , respectively. We assume that  $\mathbf{b}_i = (\mathbf{b}_{i1}^\top, \dots, \mathbf{b}_{iK}^\top)^\top$  takes into account the association within and between the multiple longitudinal markers such that  $\mathbf{b}_i \sim N(\mathbf{0}, \boldsymbol{\Sigma})$ , and  $\boldsymbol{\Sigma}$  is a  $q \times q$  covariance matrix, where  $q = \sum_{k=1}^K q_k$ . It is assumed that  $\varepsilon_{ijk}$  is independent of  $\mathbf{b}_{ik}$ ,  $i = 1, \dots, K$ .

### 2.2 Competing risks sub-model

For each of the  $L$  causes, a cause-specific proportional hazard model is postulated. The risk of an event is assumed to be a function of the subject-specific linear predictors  $\eta_{ik}(t | \boldsymbol{\beta}_k, \mathbf{b}_{ik})$  and of time-invariant covariates as follows [8]:

$$\lambda_{il}(t | \boldsymbol{\omega}_i, \mathbf{b}_i) = \lambda_{0l}(t) \exp\{\boldsymbol{\gamma}_l^\top \boldsymbol{\omega}_i + \sum_{k=1}^K \alpha_{lk} \eta_{ik}(t | \boldsymbol{\beta}_k, \mathbf{b}_{ik})\}, l = 1, 2, \dots, L, \quad (3)$$

where  $\lambda_{0l}(t)$  denotes the baseline hazard function for the  $l$ th cause,  $\boldsymbol{\omega}_{il}$  is a  $p_l^\gamma$  vector of covariates with corresponding regression coefficients  $\boldsymbol{\gamma}_l$ , and  $\boldsymbol{\alpha}_l = (\alpha_{l1}, \dots, \alpha_{lK})^\top$  represents the vector of association parameters between the longitudinal markers and cause  $l$ . There are different approaches for specifying the baseline hazard function in joint modeling [8]. The methodology is not restricted to a specific form of the baseline hazard, and we consider a piecewise constant baseline hazard [35]. To specify

a piecewise constant baseline hazard, we construct a finite partition of the time axis as  $0 = \xi_0 < \xi_1 < \dots < \xi_{\mathcal{K}} < \infty$ , such that all observed event or censoring times fall within the last interval, i.e.,  $T_i \leq \xi_{\mathcal{K}}$  for all  $i = 1, \dots, N$ . The intervals are defined as  $(\xi_{\kappa-1}, \xi_{\kappa}]$ ,  $\kappa = 1, \dots, \mathcal{K}$ , and the baseline hazard is assumed constant within each interval,  $\lambda_{0l}(t) = \lambda_{\kappa l}$  for  $t \in (\xi_{\kappa-1}, \xi_{\kappa}]$ . In practice,  $\xi_{\mathcal{K}}$  is chosen slightly larger than the maximum observed time, and the number of intervals  $\mathcal{K}$  is selected to balance model flexibility and parameter stability, often based on quantiles of the observed times or information criteria [36].

### 2.3 Parameter estimation of the multi-marker joint model

We define  $\boldsymbol{\psi}_k = (\boldsymbol{\beta}_k^\top, \sigma_k^2)^\top$ , where  $\boldsymbol{\beta}_k$  are the fixed-effect coefficients and  $\sigma_k^2$  the residual variance for the  $k$ th longitudinal marker. For the competing risks sub-model,  $\boldsymbol{\Upsilon} = (\boldsymbol{\gamma}_1^\top, \dots, \boldsymbol{\gamma}_L^\top, \boldsymbol{\alpha}_1^\top, \dots, \boldsymbol{\alpha}_L^\top, \lambda_{11}, \dots, \lambda_{\mathcal{K}L})^\top$ , where  $\boldsymbol{\gamma}_l$  are regression coefficients,  $\boldsymbol{\alpha}_l$  are association parameters, and  $\lambda_{\kappa l}$  are piecewise constant baseline hazards for cause  $l$ . We define the stacked parameter vector for the longitudinal sub-models as  $\boldsymbol{\psi} = (\boldsymbol{\psi}_1^\top, \dots, \boldsymbol{\psi}_K^\top)^\top$ , and the vector of all observed longitudinal data as  $\mathbf{y} = (\mathbf{y}_1^\top, \dots, \mathbf{y}_N^\top)^\top$ , where  $\mathbf{y}_i = (\mathbf{y}_{i1}^\top, \dots, \mathbf{y}_{iK}^\top)^\top$  is the vector of all repeated measurements for subject  $i$ , with  $\mathbf{y}_{ik} = (y_{i1k}, \dots, y_{in_{ik}})^\top$  denoting the measurements of marker  $k$ . Furthermore,  $t_i$  denotes the observed event or censoring time for subject  $i$ , i.e., the realization of the random variable  $T_i = \min(T_{i1}^*, \dots, T_{iL}^*, C_i)$ , and  $\mathbf{y}_i$  represents the realization of the corresponding random vector of longitudinal outcomes  $\mathbf{Y}_i = \{Y_{ijk} : j = 1, \dots, n_i; k = 1, \dots, K\}$ . Let  $\mathbf{t} = (t_1, \dots, t_N)^\top$  and  $\boldsymbol{\delta} = (\delta_1, \dots, \delta_N)^\top$ . The joint likelihood function for models (1) and (3) is

$$\begin{aligned} \mathbb{L}(\boldsymbol{\psi}, \boldsymbol{\Upsilon}, \boldsymbol{\Sigma} \mid \mathbf{y}, \mathbf{t}, \boldsymbol{\delta}) &= \prod_{i=1}^N \int \underbrace{\prod_{k=1}^K p(\mathbf{y}_{ik} \mid \mathbf{b}_{ik}, \boldsymbol{\psi}_k)}_{\text{longitudinal sub-model}} \\ &\times \underbrace{p(t_i, \delta_i \mid \boldsymbol{\omega}_i, \mathbf{b}_i, \boldsymbol{\Upsilon})}_{\text{competing risks sub-model}} \underbrace{p(\mathbf{b}_i \mid \boldsymbol{\Sigma})}_{\text{random effects}} d\mathbf{b}_i \\ &= \prod_{i=1}^N \int \left( \prod_{k=1}^K \prod_{j=1}^{n_i} \phi(y_{ijk}; \eta_{ik}(s_{ijk} \mid \boldsymbol{\beta}_k, \mathbf{b}_{ik}), \sigma_k^2) \right) \\ &\times \left( \prod_{l=1}^L \lambda_{il}(t_i \mid \boldsymbol{\omega}_i, \mathbf{b}_i, \boldsymbol{\Upsilon})^{I(\delta_i=l)} \exp \left\{ - \sum_{l=1}^L \Lambda_{il}(t_i \mid \boldsymbol{\omega}_i, \mathbf{b}_i, \boldsymbol{\Upsilon}) \right\} \right) \\ &\times \phi_q(\mathbf{b}_i; \mathbf{0}, \boldsymbol{\Sigma}) d\mathbf{b}_i, \end{aligned} \quad (4)$$

where  $\Lambda_{il}(t \mid \boldsymbol{\omega}_i, \mathbf{b}_i)$  is the cumulative hazard function of Equation (3), and  $\phi(x; \mu, \sigma^2)$  and  $\phi_q(\mathbf{x}; \boldsymbol{\mu}, \boldsymbol{\Sigma})$  denote the densities of the univariate and  $q$ -variate normal distributions, respectively. Also,  $I(\delta_i = l)$  denotes the indicator function, defined

as

$$I(\delta_i = l) = \begin{cases} 1, & \text{if } \delta_i = l, \\ 0, & \text{otherwise.} \end{cases}$$

It ensures that the hazard of cause  $l$  only contributes to the likelihood if subject  $i$  experiences event  $l$ ; otherwise, it contributes 1.

In the frequentist paradigm, parameter estimation can be computed by maximizing (4), which involves the use of numerical integration [37, 38]. This integration will be more challenging when the number of outcomes increases. In the Bayesian paradigm [39–42], parameter estimation is based on the joint posterior distribution

$$\begin{aligned} \pi(\boldsymbol{\psi}, \boldsymbol{\Upsilon}, \mathbf{b}, \boldsymbol{\Sigma} \mid \mathbf{y}, \mathbf{t}, \boldsymbol{\delta}) &\propto \prod_{i=1}^N \left[ \prod_{k=1}^K \prod_{j=1}^{n_i} p(y_{ijk} \mid \mathbf{b}_{ik}, \boldsymbol{\psi}_k) p(\boldsymbol{\psi}_k) \right] \\ &\times \prod_{l=1}^L \lambda_{il}(t_i \mid \boldsymbol{\omega}_i, \mathbf{b}_i, \boldsymbol{\Upsilon})^{I(\delta_i=l)} \exp \left\{ - \sum_{l=1}^L \Lambda_{il}(t_i \mid \boldsymbol{\omega}_i, \mathbf{b}_i, \boldsymbol{\Upsilon}) \right\} \\ &\times \phi_q(\mathbf{b}_i; \mathbf{0}, \boldsymbol{\Sigma}) p(\boldsymbol{\Upsilon}) p(\boldsymbol{\Sigma}), \end{aligned} \quad (5)$$

where  $\mathbf{b} = (\mathbf{b}_1^\top, \dots, \mathbf{b}_N^\top)^\top$  is the stacked vector of random effects for all subjects, with  $\mathbf{b}_i = (\mathbf{b}_{i1}^\top, \dots, \mathbf{b}_{iK}^\top)^\top$  representing the random effects for the  $K$  longitudinal markers of subject  $i$ . The prior distributions are chosen to be weakly informative to allow the data to dominate the posterior while ensuring computational stability: Regression coefficients  $\boldsymbol{\beta}_k$  and association parameters  $\boldsymbol{\alpha}_l$ : zero-mean normal distributions with large variance; Residual variances  $\sigma_k^2$ : inverse gamma distributions with small shape and scale parameters; Random effects covariance  $\boldsymbol{\Sigma}$ : inverse Wishart distribution with degrees of freedom equal to the dimension of  $\mathbf{b}_i$  and identity scale matrix; Baseline hazard parameters  $\lambda_{kl}$ : gamma distributions with mean 1 and large variance.

These choices provide sufficient flexibility while maintaining numerical stability, avoiding the potential convergence and identifiability issues associated with fully non-informative priors [41, 43].

In the next section, we introduce our proposed two-stage approach for variable selection of longitudinal markers and covariates in a Bayesian paradigm.

## 2.4 Two-stage joint modeling of multiple longitudinal measurements and competing risks

The proposed method adopts a two-stage approach for variable selection in joint modeling, targeting the selection of markers (or time-varying covariates) and time-invariant covariates. This approach is specifically designed for handling multiple longitudinal markers and time-to-event outcomes, with the primary goal of avoiding bias caused by informative dropouts. This relies on the idea of TSJM approach of [17] but considering competing risks and replacing the estimation of a Cox model by partial likelihood in the second stage by a fully Bayesian approach allowing variable selection.

The first stage involves estimating  $K$  one-marker joint models for the competing risks and each marker. In the second stage, we estimate cause-specific proportional hazard

models including the time-invariant explanatory variables and the predicted current values of the linear predictor of each longitudinal markers obtained from stage 1. Therefore, the approach consists of two stages, outlined as follows:

*Stage 1* For each  $k, k = 1, \dots, K$ , estimate the joint model for the longitudinal marker  $k$  and competing risks. The one-marker JMs are estimated using the joint posterior distribution given by Equation (5) for  $K = 1$ . Then, predict the random effects  $\hat{\mathbf{b}}_{ik}$  and the linear predictor  $\eta_{ik}(t|\hat{\boldsymbol{\beta}}_k, \hat{\mathbf{b}}_{ik})$ , for marker  $k$  using the empirical mean of the posterior distribution  $(\mathbf{b}_{ik}|\mathbf{y}_{ik}, t_i, \delta_i, \hat{\boldsymbol{\theta}}_k)$ , where  $\hat{\boldsymbol{\theta}}_k$  represents the estimated parameters for the one-marker joint model for the  $k$ th longitudinal marker. This first stage allow the estimation of  $\eta_{ik}(t|\hat{\boldsymbol{\beta}}_k, \hat{\mathbf{b}}_{ik})$  without the bias due to informative dropout but neglecting the correlation between the markers.

*Stage 2* In the second stage, the values of  $\eta_{ik}(t|\hat{\boldsymbol{\beta}}_k, \hat{\mathbf{b}}_{ik})$  are included as time-varying covariates in a proportional hazard model to estimate parameters  $\boldsymbol{\gamma}$  and  $\boldsymbol{\alpha}_k$ , as well as the baseline hazard from (3). The cumulative hazard function of (3) can be approximated using Gaussian quadrature [44, 45]. In the Bayesian paradigm, the following joint posterior distribution is considered:

$$\begin{aligned} \pi(\boldsymbol{\lambda}, \boldsymbol{\alpha} | \mathbf{t}, \boldsymbol{\delta}, \hat{\mathbf{b}}) &\propto \prod_{i=1}^N \prod_{l=1}^L [\lambda_{il}(t_i|\boldsymbol{\omega}_i, \hat{\mathbf{b}}_i, \boldsymbol{\Upsilon}_l)]^{I(\delta_i=l)} \\ &\times \exp\left(-\sum_{l=1}^L \Lambda_{il}(t_i|\boldsymbol{\omega}_i, \hat{\mathbf{b}}_i, \boldsymbol{\Upsilon}_l)\right) \times p(\boldsymbol{\Upsilon}), \end{aligned} \quad (6)$$

where  $\boldsymbol{\Upsilon}_l = (\boldsymbol{\gamma}_l^\top, \boldsymbol{\alpha}_l^\top, \boldsymbol{\lambda}_l^\top)^\top$ , with  $\boldsymbol{\lambda}_l = (\lambda_{l1}, \dots, \lambda_{l\mathcal{K}})^\top$  denoting the vector of piecewise-constant baseline hazards for cause  $l$ . We also define  $\boldsymbol{\alpha} = (\boldsymbol{\alpha}_1^\top, \dots, \boldsymbol{\alpha}_L^\top)^\top$  and  $\boldsymbol{\lambda} = (\lambda_{11}, \dots, \lambda_{\mathcal{K}L})^\top$ . Furthermore,  $\boldsymbol{\Upsilon}$  is as defined in Equation (4), and the prior distributions for all unknown parameters are the same as those specified for Equation (5).

## 2.5 Bayesian variable selection

As above, we consider the prior distributions  $\boldsymbol{\beta}_k \sim N_{p_k}(\mathbf{0}, c\mathbf{I}_{p_k})$ , where  $\mathbf{0}$  is a  $p_k$ -dimensional vector of zeros,  $\mathbf{I}_{p_k}$  is the  $p_k \times p_k$  identity matrix, and  $c$  is a large positive constant,  $\sigma_k^2 \sim \Pi(a_\sigma, b_\sigma)$ ,  $\boldsymbol{\Sigma} \sim \text{IWishart}(\boldsymbol{\nu}, \nu)$  and  $\lambda_{l\kappa} \sim \Gamma(a_{l\kappa}, b_{l\kappa})$ ,  $\kappa = 1, \dots, \mathcal{K}$ ,  $l = 1, \dots, L$ . Our purpose is to implement variable selection for the regression coefficients  $\boldsymbol{\gamma}_l$ ,  $l = 1, \dots, L$  of the cause-specific hazard model (3) and the association parameters  $\boldsymbol{\alpha}_l$ ,  $l = 1, \dots, L$  of (3). Therefore, we consider two different prior distributions, including continuous spike and Dirac spike, for them.

A key advantage of the Bayesian variable selection approach is that the posterior distributions of the coefficients  $\boldsymbol{\gamma}_l$  and  $\boldsymbol{\alpha}_l$  naturally account for both parameter uncertainty and the uncertainty arising from the variable selection process itself [46–48]. Consequently, the posterior means and standard deviations provide valid measures of effect size and uncertainty without the need to re-estimate the model using only the selected variables, as is commonly done in frequentist post-selection procedures. This property ensures that credible intervals and inference fully reflect the selection process.

### 2.5.1 Continuous spike

The continuous spike [CS, 21, 22] prior for  $\gamma_l = (\gamma_{l1}, \dots, \alpha_{p_l^{\gamma_l}})^\top$  is given by

$$\begin{aligned} \gamma_{lj} | \zeta_{lj}, \sigma_{\gamma_{lj}}^2, \tau_{\gamma_{lj}}^2 &\stackrel{\text{ind}}{\sim} (1 - \zeta_{lj})N(0, \sigma_{\gamma_{lj}}^2) + \zeta_{lj}N(0, \tau_{\gamma_{lj}}^2), \quad \sigma_{\gamma_{lj}}^2 > \tau_{\gamma_{lj}}^2 > 0, \quad l = 1, \dots, L, \quad j = 1, \dots, p_l^\gamma, \\ \zeta_{lj} | \pi_{\gamma_{lj}} &\stackrel{\text{ind}}{\sim} \text{Ber}(\pi_{\gamma_{lj}}), \\ \pi_{\gamma_{lj}} | a_{\gamma_{lj}}, b_{\gamma_{lj}} &\stackrel{\text{ind}}{\sim} \text{Beta}(a_{\gamma_{lj}}, b_{\gamma_{lj}}), \\ \sigma_{\gamma_{jk}}^2 | a_{\sigma_{\gamma_{jk}}^2}, b_{\sigma_{\gamma_{jk}}^2} &\stackrel{\text{ind}}{\sim} \text{II}(a_{\sigma_{\gamma_{jk}}^2}, b_{\sigma_{\gamma_{jk}}^2}). \end{aligned} \quad (7)$$

Also, the CS prior for the association parameter  $\alpha_l = (\alpha_{l1}, \dots, \alpha_{lK})^\top$  is given by

$$\begin{aligned} \alpha_{lk} | \zeta_{lk}, \sigma_{\alpha_{lk}}^2, \tau_{\alpha_{lk}}^2 &\stackrel{\text{ind}}{\sim} (1 - \zeta_{lk})N(0, \sigma_{\alpha_{lk}}^2) + \zeta_{lk}N(0, \tau_{\alpha_{lk}}^2), \quad \sigma_{\alpha_{lk}}^2 > \tau_{\alpha_{lk}}^2 > 0, \quad k = 1, \dots, K, \\ \zeta_{lk} | \pi_{\alpha_{lk}} &\stackrel{\text{ind}}{\sim} \text{Ber}(\pi_{\alpha_{lk}}), \\ \pi_{\alpha_{lk}} | a_{\alpha_{lk}}, b_{\alpha_{lk}} &\stackrel{\text{ind}}{\sim} \text{Beta}(a_{\alpha_{lk}}, b_{\alpha_{lk}}), \\ \sigma_{\alpha_{lk}}^2 | a_{\sigma_{\alpha_{lk}}^2}, b_{\sigma_{\alpha_{lk}}^2} &\stackrel{\text{ind}}{\sim} \text{II}(a_{\sigma_{\alpha_{lk}}^2}, b_{\sigma_{\alpha_{lk}}^2}). \end{aligned} \quad (8)$$

where,  $\tau_{\gamma_{lj}}^2$  in (7) and  $\tau_{\alpha_{lk}}^2$  in (8) are a small fixed value (e.g.,  $10^{-3}$  or  $10^{-4}$ ) and represents a spike prior. The latent variable  $\zeta_{lj}$  in (7) (or  $\zeta_{lk}$  in (8)) is considered to account for the significance of the parameter. For example, if  $\zeta_{jk} = 0$ , then the distribution of  $\zeta_{lk}, \sigma_{\alpha_{lk}}^2, \tau_{\alpha_{lk}}^2$  will be  $N(0, \sigma_{\alpha_{lk}}^2)$ , and can be considered as significant. This leads us to have a slab prior. A graphical example of CS prior can be found in panel (a) of Figure 1.

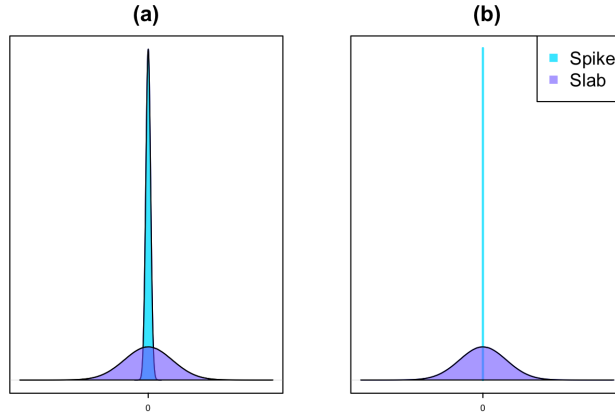


**Fig. 1** An example of continuous spike prior (Panel a) and Dirac spike prior (Panel b).

### 2.5.2 Dirac spike

We exploit a Dirac spike-and-slab prior [DS, 21, 23] similar to that proposed by [49]. For this purpose, the DS prior for  $\gamma_l$  is given by

$$\begin{aligned} \gamma_{lj} | \pi_{\gamma_{lj}}, \sigma_{\gamma_{lj}}^2 &\stackrel{ind}{\sim} (1 - \pi_{\gamma_{lj}}) N(0, \sigma_{\gamma_{lj}}^2) + \pi_{\gamma_{lj}} \delta_0(\gamma_{lj}), \quad \sigma_{\gamma_{lj}}^2 > 0, \quad l = 1, \dots, L, \quad j = 1, \dots, p_l^\gamma, \\ \pi_{\gamma_{lj}} | a_{\gamma_{lj}}, b_{\gamma_{lj}} &\stackrel{ind}{\sim} \text{Beta}(a_{\gamma_{lj}}, b_{\gamma_{lj}}), \\ \sigma_{\gamma_{lj}}^2 | a_{\sigma_{\gamma_{lj}}^2}, b_{\sigma_{\gamma_{lj}}^2} &\stackrel{ind}{\sim} \text{IG}(a_{\sigma_{\gamma_{lj}}^2}, b_{\sigma_{\gamma_{lj}}^2}). \end{aligned} \quad (9)$$

where  $\delta_0(\gamma_{lj})$  represents a point mass at  $0 \in \mathbb{R}$ . It is defined as  $\delta_0(\gamma_{lj}) = 1$  when  $\gamma_{lj} = 0$  and  $\delta_0(\gamma_{lj}) = 0$  when  $\gamma_{lj}$  is non-zero, i.e.,  $\gamma_{lj} \neq 0$ . Also, the DS prior for the association parameter  $\alpha$  is given by

$$\begin{aligned} \alpha_{lk} | \pi_{\alpha_{lk}}, \sigma_{\alpha_{lk}}^2 &\stackrel{ind}{\sim} (1 - \pi_{\alpha_{lk}}) N(0, \sigma_{\alpha_{lk}}^2) + \pi_{\alpha_{lk}} \delta_0(\alpha_{lk}), \quad \sigma_{\alpha_{lk}}^2 > 0, \quad k = 1, \dots, K, \\ \pi_{\alpha_{lk}} | a_{\alpha_{lk}}, b_{\alpha_{lk}} &\stackrel{ind}{\sim} \text{Beta}(a_{\alpha_{lk}}, b_{\alpha_{lk}}), \\ \sigma_{\alpha_{lk}}^2 | a_{\sigma_{\alpha_{lk}}^2}, b_{\sigma_{\alpha_{lk}}^2} &\stackrel{ind}{\sim} \text{IG}(a_{\sigma_{\alpha_{lk}}^2}, b_{\sigma_{\alpha_{lk}}^2}). \end{aligned} \quad (10)$$

A graphical example of the DS prior can be found in panel (b) of Figure 1. For implementing Bayesian inference, a block Gibbs sampler is used in conjunction with the Metropolis-Hastings algorithm. For this purpose, we require all of the full conditional distributions. The Markov Chain Monte Carlo (MCMC) sampling is performed using ‘‘JAGS’’ [50, 51] and the R2jags [52] package is utilized as an interface between R and JAGS. The package automatically computes the full conditional posterior distributions for all parameters and models. We refer to this approach as Variable Selection for Joint Modeling (VSJM). The methodology has been implemented in the R package VSJM.

## 2.6 Statistical inference

To select significant variables in the covariates of the cause-specific hazard model and by considering Equation (7) or (9), the following hypothesis tests are conducted:

$$\begin{cases} H_{0lj}^\gamma : \gamma_{lj} = 0 \\ H_{1lj}^\gamma : \gamma_{lj} \neq 0 \end{cases}, \quad j = 1, \dots, p_l^\gamma, l = 1, \dots, L, \quad (11)$$

Also, to select significant longitudinal markers based on the association parameters and by considering Equation (8) or (10), the following hypothesis tests are considered:

$$\begin{cases} H_{0lk}^\alpha : \alpha_{lk} = 0 \\ H_{1lk}^\alpha : \alpha_{lk} \neq 0 \end{cases}, \quad k = 1, \dots, K, l = 1, \dots, L, \quad (12)$$

In practice, when implementing the hypotheses (11) and (12) for CS, it is possible to consider the following equivalent hypotheses, respectively:

$$\begin{cases} H_{0lj}^\zeta : \zeta_{lj} = 0 \\ H_{1lj}^\zeta : \zeta_{lj} \neq 0 \end{cases}, \quad j = 1, \dots, p_l^\zeta, l = 1, \dots, L, \quad (13)$$

$$\begin{cases} H_{0lk}^\alpha : \zeta_{lk} = 0 \\ H_{1lk}^\alpha : \zeta_{lk} \neq 0 \end{cases}, \quad k = 1, \dots, K, l = 1, \dots, L, . \quad (14)$$

We consider two different Bayesian testing approaches for evaluating these hypotheses: a local Bayesian false discovery rate [53] and a Bayes factor [54].

### 2.6.1 Continuous spike

#### Local Bayesian false discovery rate

Let  $\mathcal{D}$  denote the data in the study. The set of unknown parameters of the CS model is denoted as  $\boldsymbol{\theta}$ . Let  $P(H_{0k}|\mathcal{D})$  represent the posterior probability of the null hypothesis. This is the probability of making a false discovery for a significant covariate, which is called the local Bayesian false discovery rate for  $\mathcal{D}$  (denoted by  $lBFDR$ ) by Efron [53]. The small values of  $lBFDR$  indicate strong evidence for the presence of a significant covariate. For computing  $lBFDR$  of Equation (13), we obtain

$$\begin{aligned} lBFDR_{lj}^\gamma &= P(H_{0lj}^\gamma|\mathcal{D}) = P(\zeta_{lj} = 0|\mathcal{D}) \\ &\approx \frac{1}{M} \sum_{m=1}^M I(\zeta_{lj} = 0|\mathcal{D}, \boldsymbol{\theta}^{(m)}), \end{aligned}$$

where  $I(\zeta_{lj} = 0|\mathcal{D}, \boldsymbol{\theta}^{(m)})$  is an indicator function and  $\boldsymbol{\theta}^{(m)}$  denotes the  $m^{th}$ ,  $m = 1, \dots, M$ , generated sample of  $\boldsymbol{\theta}$  using the Gibbs sampler.

The  $lBFDR$  is a procedure for investigating the null hypothesis. It is an empirical Bayes version of the methodology proposed by [55]. This approach focuses on densities instead of tail areas [56–58]. Efron [58] demonstrated that the false discovery rate control rule proposed by [55] can be expressed in terms of empirical Bayes. They also showed that the desired control level (referred to as  $\alpha[= 0.05]$ ) for Benjamini-Hochberg testing of single tests can be regarded as the desired control level for local Bayes false discovery rate ( $lBFDR$ ) as well. Based on Remark B of [58], if the value of  $lBFDR$  is not greater than 0.05 (the desired control level), the null hypothesis will be rejected. In fact, the interpretation of the  $lBFDR$  value is analogous to the frequentist's p-value.  $lBFDR$  values less than a specified level (e.g., 0.05) of significance provide stronger evidence against the null hypothesis [59, 60]. The value of 0.05 in the context of variable selection is also considered a threshold for  $lBFDR$  by [61] and [62]. Thus, a local Bayesian false discovery rate of 0.05 is considered in this paper.

#### Bayes factor

The Bayes factor for testing (13) is defined as

$$\begin{aligned} BF_{lj}^\gamma &= \frac{P(H_{1lj}^\gamma|\mathcal{D})/P(H_{1lj}^\gamma)}{P(H_{0lj}^\gamma|\mathcal{D})/P(H_{0lj}^\gamma)} \\ &= \frac{P(\zeta_{lj} \neq 0|\mathcal{D})/P(\zeta_{lj} \neq 0)}{P(\zeta_{lj} = 0|\mathcal{D})/P(\zeta_{lj} = 0)}, \end{aligned}$$

which describes the evidence of  $H_{1k}$  against  $H_{0k}$ . Note that  $P(\zeta_{lj} = 1) = E[\pi_{\gamma_{lj}}] = \frac{a_{\gamma_{lj}}}{a_{\gamma_{lj}} + b_{\gamma_{lj}}}$  as  $\zeta_{11}, \dots, \zeta_{Lp_L^\gamma}$  are assumed independent. Hence,

$$P(\zeta_{lj} = 0) = \frac{b_{\gamma_{lj}}}{a_{\gamma_{lj}} + b_{\gamma_{lj}}}.$$

Also, since  $lBFDR_{lj}^\gamma = P(H_{0lj}^\gamma | \mathcal{D})$ ,

$$BF_{lj}^\gamma = \frac{1 - lBFDR_{lj}^\gamma}{lBFDR_{lj}^\gamma} \times \frac{b_{\gamma_{lj}}}{a_{\gamma_{lj}}}. \quad (15)$$

Unlike  $lBFDR$ , a large value of  $BF$  indicates strong evidence in favor of  $H_1$ . Also, a widely cited table is provided by [54]. This table is based on  $\log_{10}(BF_k)$  and can be used to quantify the support that one model has over another.

All comments mentioned above can also be applied to the hypothesis testing of Equations (14).

### 2.6.2 Dirac spike

The strategy for performing  $lBFDR$  and  $BF$  for DS is to define indicator variables as  $\Psi_{lj}^\gamma, j = 1, \dots, p_l^\gamma, l = 1, \dots, L$ , and  $\Psi_{lk}^\alpha, k = 1, \dots, K$  such that

$$\Psi_{lj}^\gamma = \begin{cases} 1 & \text{if } \gamma_{lj} \neq 0 \\ 0 & \text{if } \gamma_{lj} = 0 \end{cases},$$

$$\Psi_{lk}^\alpha = \begin{cases} 1 & \text{if } \alpha_{lk} \neq 0 \\ 0 & \text{if } \alpha_{lk} = 0 \end{cases}.$$

By considering these indicator variables, all of those described for the CS can also be used for the DS.

## 3 Dynamic predictions

### 3.1 Dynamic predictions from VSJM

The joint modeling of longitudinal measurements and time-to-event outcomes is a popular methodology for calculating dynamic prediction (DP). The DP represents the risk predictions for subject  $i$  who has survived up to time point  $s$ , taking into account longitudinal measurements and other information available until time  $s$ . Consider the notation described in Section 2. Let the proposed joint models be fitted to a random sample, which is referred to as training data. For validation purposes, we are interested in predicting the risk of subjects in a new set of data called the validation set. The longitudinal measurements until time  $s$  are denoted by  $\mathcal{Y}_i(s)$  and given by  $\{Y_{ik}(s_{ijk}); 0 \leq s_{ijk} \leq s, j = 1, \dots, n_i, k = 1, \dots, K\}$ . Additionally, the vector of available explanatory variables until time  $s$  is  $\mathcal{X}_i(s)$  and given by  $\{\mathbf{w}_i, \mathbf{X}_{ik}(s_{ijk}); 0 \leq s_{ijk} \leq s, j = 1, \dots, n_i, k = 1, \dots, K\}$ . Let  $\delta_i = 1$  denote the

event of interest, then, for the landmark time  $s$  and the prediction window  $t$ , the risk probability is as follows:

$$\pi_i(s+t | s) = P(s \leq T_i^* < s+t, \delta_i = 1 | T_i^* > s, \mathcal{Y}_i(s), \mathcal{X}_i(s); \boldsymbol{\theta}), \quad (16)$$

where  $\boldsymbol{\theta}$  is a vector of all unknown parameters of the model, including  $\boldsymbol{\theta}_k$  which is estimated at stage 1, and  $\boldsymbol{\Upsilon}$  which is estimated at stage 2, and  $T_i^*$  represents the true event time for the  $i$ th subject. The predicted probability (16) can be computed as:

$$\begin{aligned} & P\left(s \leq T_i^* < s+t, \delta_i = 1 | T_i^* > s, \mathcal{Y}_i(s), \mathcal{X}_i(s); \boldsymbol{\theta}\right) \\ &= \int \frac{P\left(s \leq T_i^* < s+t, \delta_i = 1 | \mathbf{b}_i, \mathcal{X}_i(s); \boldsymbol{\theta}\right)}{S\left(s | \mathbf{b}_i, \mathcal{X}_i(s); \boldsymbol{\theta}\right)} \\ & \quad \times f\left(\mathbf{b}_i | T_i^* > s, \mathcal{Y}_i(s), \mathcal{X}_i(s); \boldsymbol{\theta}\right) d\mathbf{b}_i \end{aligned} \quad (17)$$

where  $S(\cdot)$  represents the survival probability to survive to both events given random effects. The first order approximation for estimating this quantity [7, 17] is given as follows:

$$\hat{\pi}_i(s+t | s) = \frac{\int_s^{s+t} \exp\{-\sum_{l=1}^L \Lambda_l(u | \hat{\mathbf{b}}_i, \mathcal{X}_i(s); \hat{\boldsymbol{\theta}})\} \lambda_1(u | \hat{\mathbf{b}}_i, \mathcal{X}_i(s); \hat{\boldsymbol{\theta}}) du}{\exp\{-\sum_{l=1}^L \Lambda_l(s | \hat{\mathbf{b}}_i, \mathcal{X}_i(s); \hat{\boldsymbol{\theta}})\}},$$

where  $\hat{\boldsymbol{\theta}} = \{\hat{\boldsymbol{\theta}}_1, \dots, \hat{\boldsymbol{\theta}}_K, \hat{\boldsymbol{\Upsilon}}\}$  are estimated based on the training data. To predict  $\hat{\mathbf{b}}_i$ , we consider the one-marker joint models for each marker and predict the  $p_k$ -dimensional random effect  $\mathbf{b}_{ik}$  given  $(T_i^* > s, \mathcal{Y}_i(s), \mathcal{X}_i(s), \boldsymbol{\theta}_k)$ . This is denoted by  $\hat{\mathbf{b}}_{ik}$ , where  $\hat{\boldsymbol{\theta}}_k$  represents the estimated parameters for the one-marker joint model in the first stage of VSJM. Merge the predicted random effects to obtain the  $p = \sum_{k=1}^K p_k$ -dimensional predicted random effect  $\hat{\mathbf{b}}_i = (\hat{\mathbf{b}}_{i1}, \dots, \hat{\mathbf{b}}_{iK})$ .

For Monte-Carlo approximation of (17), we follow the same strategy as those discussed in [63]. For this aim, consider a realization of the generated MCMC sample for estimating the unknown parameters from the one-marker JM for marker  $k$  in the training data, denoted  $\boldsymbol{\theta}_k^{(\ell)}$ ,  $\ell = 1, \dots, \mathcal{L}$ . Draw  $M$  values  $\mathbf{b}_{ik}^{(\ell, m)}$  from the posterior distribution  $(\mathbf{b}_{ik} | T_i^* > s, \mathcal{Y}_i(s), \mathcal{X}_i(s), \boldsymbol{\theta}_k^{(\ell)})$ . For  $\ell = 1, \dots, \mathcal{L}$ ,  $m = 1, \dots, M$ ,

$$\hat{\pi}_i(s+t | s)^{(\ell, m)} = \frac{\int_s^{s+t} \exp\{-\sum_{l=1}^L \Lambda_l(u | \mathbf{b}_i^{(\ell, m)}, \mathcal{X}_i(s); \boldsymbol{\theta}_k^{(\ell)})\} \lambda_1(u | \mathbf{b}_i^{(\ell, m)}, \mathcal{X}_i(s); \boldsymbol{\theta}_k^{(\ell)}) du}{\exp\{-\sum_{l=1}^L \Lambda_l(s | \mathbf{b}_i^{(\ell, m)}, \mathcal{X}_i(s); \boldsymbol{\theta}_k^{(\ell)})\}}.$$

Calculate any desired quantity from the generated chains, such as percentiles, to determine the credible interval.

## 3.2 Reducing bias in dynamic predictions from VSJM

To reduce estimation biases resulting from variable selection, we propose incorporating an additional stage to calculate dynamic predictions. After variable selection using CS or DS prior, we recommend re-estimating the proportional hazard model by substituting CS or DS with non-informative normal priors for the association parameters of the selected markers and the regression coefficients of the selected covariates. Then calculate the DP as described in Section 3.1.

## 3.3 Measures of prediction accuracy

We use the Area Under the Receiver Operating Characteristics Curve (AUC) and the Brier Score (BS) to assess the predictive performance of prediction models [64]. AUC represents the probability that the model correctly ranks a randomly chosen individual with the disease higher than a randomly chosen individual without the disease based on their predicted risks. Additionally, BS measures the prediction accuracy by quantifying the mean squared error of prediction. For censored and competing time-to-event and time-dependent markers, a non-parametric inverse probability of censoring weighted estimator of AUC and BS was proposed by [65] and utilized in this paper.

# 4 Simulation study

## 4.1 Design of simulation study

A simulation study was conducted to assess the effectiveness of the proposed VSJM approach for variable selection and risk prediction. To evaluate the effectiveness of the proposed approaches for variable selection, we examine three distinct criteria: the true positive rate (TPR), which measures the proportion of correctly selected variables among all significant variables; the false positive rate (FPR), which measures the proportion of incorrectly selected variables among all irrelevant variables; and the Matthews correlation coefficient [66] (MCC). The latter is defined as follows:

$$\text{MCC} = \frac{\text{TP} \times \text{TN} - \text{FP} \times \text{FN}}{\sqrt{(\text{TP} + \text{FP})(\text{TP} + \text{FN})(\text{TN} + \text{FP})(\text{TN} + \text{FN})}}, \quad (18)$$

where TP, TN, FP, and FN represent the number of true positives, true negatives, false positives, and false negatives, respectively. The MCC and TPR are expected to reach 1, while the FPR is expected to be close to zero for optimal performance. *BF* and *lBFDR* are used for variable selection, with the results based on a threshold of 1 for *BF* and a threshold of 0.05 for *lBFDR*.

The simulation scenarios varied based on the strength of the association between the markers and the events, the residual variances for the markers that quantify measurement error, and the correlation between the markers that is neglected in the first stage of the approach. The performance of the approaches is also evaluated based on their predictive abilities using AUC and BS. The predictive performance of the approach is compared with that of the true model using the true values of the parameters and random effects (referred to as “Real”) as well as the oracle model (true model, where

parameters are estimated by accounting for the multi-marker joint modeling). Data were generated using multi-marker joint models with  $K = 10$  longitudinal markers and a competing risks model with two causes. The longitudinal outcomes were simulated from the following model:

$$\begin{aligned} Y_{ijk} &= \eta_{ik}(s_{ijk} | \boldsymbol{\beta}_k, \mathbf{b}_{ik}) + \varepsilon_{ijk} \\ &= \beta_{0k} + \beta_{1k}s_{ijk} + b_{0ik} + b_{1ik}s_{ijk} + \varepsilon_{ijk}, \end{aligned} \quad (19)$$

where  $\varepsilon_{ijk} \sim N(0, \sigma_k^2)$ , and

$$\mathbf{b}_i = (b_{0i1}, b_{1i1}, b_{0i2}, b_{1i2}, \dots, b_{0i,10}, b_{1i,10})^\top \sim N(\mathbf{0}, \boldsymbol{\Sigma}), \quad i = 1, \dots, N.$$

For each subject  $i$ , marker  $k = 1, \dots, 10$ , and measurement index  $j$ , the observation times were defined as  $s_{ijk} \in \{0, 0.1, 0.2, \dots, 2\}$ , corresponding to equally spaced measurements over the interval  $[0, 2]$ . The fixed-effect coefficients were set to  $\boldsymbol{\beta}_k = (-0.5, 0.5)^\top$ ,  $k = 1, \dots, 10$ .

The time-to-event outcome was simulated using a cause-specific hazard model that depends on the current value of the  $K$  markers and on 24 time-invariant covariates as follows:

$$\lambda_l(t) = \lambda_{0l} \exp(\boldsymbol{\gamma}_l^\top \boldsymbol{\omega}_{il} + \sum_{k=1}^K \alpha_{lk} \eta_{ik}(t | \boldsymbol{\beta}_k, \mathbf{b}_{ik})), \quad (20)$$

where  $\boldsymbol{\omega}_{il} = (x_{1i}, w_{1i}, \dots, w_{24,i})^\top$ . Half of the covariates were independently generated from a standard normal distribution, while the others were independently generated from a binary distribution with a success probability of 0.5. To simulate time-to-event data, we apply the inverse of the cumulative hazard function [67] using the inverse probability integral transform method [68].

The covariance matrix of the random effects a structure is considered as follows:

$$\boldsymbol{\Sigma} = \begin{pmatrix} \boldsymbol{\Sigma}^* & \boldsymbol{\Sigma}^\dagger & \dots & \boldsymbol{\Sigma}^\dagger \\ & \boldsymbol{\Sigma}^* & \dots & \boldsymbol{\Sigma}^\dagger \\ & & \ddots & \vdots \\ & & & \boldsymbol{\Sigma}^* \end{pmatrix}, \quad \text{where } \boldsymbol{\Sigma}^* = \begin{pmatrix} 1 & 0.5 \\ 0.5 & 1 \end{pmatrix}, \quad \boldsymbol{\Sigma}^\dagger = \rho \begin{pmatrix} 1 & 1 \\ 1 & 1 \end{pmatrix}. \quad (21)$$

For each scenario, 100 data sets of  $N = 1000$  subjects were generated and split into a training sample of 500 subjects and a validation of 500 subjects. The investigation focused on estimating parameters on the training sample using various approaches. The performance of these approaches for risk prediction was then evaluated using the validation samples. To achieve this goal, we consider four landmark times at  $s = 0, 0.25, 0.5, 0.75$ , using  $t = 0.25$  as window for prediction.

## 4.2 Simulation with common effect for the two events

Among the 10 generated longitudinal markers and the 24 generated time-invariant covariates, only 4 markers and 4 covariates (2 Gaussian and 2 binary) were truly associated with the two event risks, sharing identical regression parameters for both events. To evaluate the impact of increasing measurement errors, association parameters, and marker correlation on the performance of the three methods, we considered different values for these parameters, as described below:

1.  $\sigma_k^2 = 0.5, 1$  for  $k = 1, 2, \dots, 10$ ,
2.  $\boldsymbol{\gamma}_l = (\gamma^*, -\gamma^*, \underbrace{0, \dots, 0}_{10}, \gamma^*, -\gamma^*, \underbrace{0, \dots, 0}_{10})^\top$ ,  $l = 1, 2$  and  $\boldsymbol{\alpha}_l = (-\alpha^*, -\alpha^*, \alpha^*, \alpha^*, 0, 0, 0, 0, 0, 0)^\top$ , where  $\gamma^* = \alpha^* = 0.5, 1$ .
3.  $\rho = 0.1, 0.7$ .

Note that the block-structured covariance matrix in (21) is positive definite for all  $\rho \in \{0.1, 0.7\}$ .

Based on the insights obtained from both Table 1, which pertains to variable selection, and Table 2, which focuses on risk prediction, regarding the performance of the VSJM, we can conclude:

- For all scenarios, AUC and BS computed on the validation set after Bayesian variable selection on the training set were close to those of the oracle model.
- Increasing the between markers correlation values tends to decrease the performance of the approach in terms of TPR, FPR, and MCC, albeit to an acceptable extent.
- Increasing the residual variance of the longitudinal markers ( $\sigma^2$ ) leads to a decrease in the performance of the approach.
- Enhanced values of association parameters and regression coefficients tend to improve the approach's performance.
- Although the predictive performance of *BF* and *lBFDR* is similar, *BF* generally outperforms *lBFDR* in terms of total variable selection, except in the easiest scenario characterized by high association and low measurement error.

**Table 1** Simulation results with identical effects for both events: Mean and standard deviation of the true positive rate (TPR), false positive rate (FPR), and Matthews Correlation Coefficient (MCC) over 100 replications. The results of DS and CS are based on a threshold of 1 for *BF* and a threshold of 0.05 for *IBFDR*.

		CS						DS					
		Total		L-Markers		Fixed covariates		Total		L-Markers		Fixed covariates	
		Est.	SD.	Est.	SD.	Est.	SD.	Est.	SD.	Est.	SD.	Est.	SD.
$\rho = 0.7, \sigma^2 = 0.5, \alpha^* = 0.5, \gamma^* = 0.5$													
<i>BF</i>	TPR	0.787	0.115	0.704	0.174	0.871	0.117	0.820	0.099	0.760	0.158	0.879	0.100
	FPR	0.028	0.023	0.049	0.060	0.021	0.025	0.053	0.029	0.097	0.088	0.040	0.032
	MCC	0.797	0.104	0.697	0.179	0.862	0.093	0.771	0.095	0.683	0.188	0.822	0.091
<i>IBFDR</i>	TPR	0.516	0.103	0.371	0.159	0.660	0.130	0.584	0.117	0.450	0.189	0.719	0.129
	FPR	0.001	0.005	0.001	0.011	0.001	0.005	0.005	0.010	0.012	0.030	0.003	0.008
	MCC	0.664	0.076	0.494	0.157	0.780	0.088	0.704	0.087	0.540	0.179	0.813	0.089
$\rho = 0.1, \sigma^2 = 0.5, \alpha^* = 0.5, \gamma^* = 0.5$													
<i>BF</i>	TPR	0.941	0.054	1.000	0.000	0.881	0.109	0.947	0.054	1.000	0.000	0.894	0.108
	FPR	0.024	0.021	0.024	0.044	0.024	0.024	0.037	0.030	0.040	0.056	0.036	0.034
	MCC	0.913	0.051	0.973	0.050	0.860	0.090	0.892	0.069	0.954	0.063	0.840	0.109
<i>IBFDR</i>	TPR	0.844	0.064	1.000	0.000	0.688	0.127	0.858	0.056	1.000	0.000	0.717	0.112
	FPR	0.001	0.004	0.001	0.011	0.001	0.005	0.003	0.007	0.006	0.021	0.002	0.008
	MCC	0.895	0.042	0.998	0.013	0.800	0.083	0.900	0.042	0.994	0.024	0.814	0.078
$\rho = 0.1, \sigma^2 = 1, \alpha^* = 0.5, \gamma^* = 0.5$													
<i>BF</i>	TPR	0.929	0.058	1.000	0.000	0.858	0.116	0.939	0.057	1.000	0.000	0.877	0.114
	FPR	0.025	0.022	0.028	0.043	0.024	0.027	0.041	0.029	0.062	0.067	0.034	0.035
	MCC	0.903	0.054	0.967	0.050	0.848	0.095	0.880	0.066	0.930	0.073	0.834	0.113
<i>IBFDR</i>	TPR	0.828	0.051	0.995	0.025	0.660	0.104	0.853	0.053	0.998	0.018	0.708	0.112
	FPR	0.003	0.009	0.005	0.020	0.003	0.011	0.002	0.006	0.005	0.020	0.001	0.005
	MCC	0.879	0.038	0.990	0.030	0.775	0.079	0.899	0.037	0.992	0.027	0.813	0.074
$\rho = 0.1, \sigma^2 = 0.5, \alpha^* = 1, \gamma^* = 1$													
<i>BF</i>	TPR	0.999	0.009	1.000	0.000	0.998	0.018	0.999	0.009	1.000	0.000	0.998	0.018
	FPR	0.035	0.026	0.037	0.051	0.034	0.031	0.060	0.039	0.057	0.070	0.061	0.043
	MCC	0.933	0.048	0.958	0.058	0.914	0.075	0.890	0.064	0.936	0.077	0.856	0.088
<i>IBFDR</i>	TPR	0.989	0.030	1.000	0.000	0.978	0.060	0.988	0.025	1.000	0.000	0.975	0.051
	FPR	0.003	0.008	0.002	0.012	0.003	0.008	0.007	0.012	0.008	0.025	0.007	0.013
	MCC	0.987	0.026	0.998	0.014	0.978	0.047	0.977	0.032	0.990	0.029	0.965	0.053
$\rho = 0.1, \sigma^2 = 1, \alpha^* = 1, \gamma^* = 1$													
<i>BF</i>	TPR	0.996	0.016	1.000	0.000	0.992	0.032	1.000	0.000	1.000	0.000	1.000	0.000
	FPR	0.038	0.026	0.053	0.056	0.034	0.027	0.062	0.025	0.081	0.056	0.057	0.029
	MCC	0.924	0.045	0.939	0.063	0.908	0.064	0.885	0.041	0.908	0.060	0.862	0.062
<i>IBFDR</i>	TPR	0.979	0.038	1.000	0.000	0.958	0.076	0.981	0.029	1.000	0.000	0.963	0.058
	FPR	0.003	0.007	0.006	0.021	0.002	0.006	0.010	0.011	0.019	0.036	0.007	0.011
	MCC	0.981	0.028	0.994	0.025	0.970	0.051	0.968	0.027	0.977	0.042	0.958	0.046

**Table 2** Simulation results with identical effects for both events: Mean and standard deviation of AUC and Brier score computed for landmark times  $s = 0, 0.25, 0.5, 0.75$  and prediction window of 0.25.

		Real		Oracle		CS				DS			
						<i>BF</i>		<i>IBFDR</i>		<i>BF</i>		<i>IBFDR</i>	
	s	Est.	SD.	Est.	SD.	Est.	SD.	Est.	SD.	Est.	SD.	Est.	SD.
$\rho = 0.7, \sigma^2 = 0.5, \alpha^* = 0.5, \gamma^* = 0.5$													
AUC	0	0.789	0.026	0.770	0.028	0.724	0.033	0.711	0.036	0.723	0.033	0.712	0.038
	0.25	0.737	0.051	0.719	0.048	0.685	0.052	0.665	0.051	0.685	0.051	0.674	0.051
	0.5	0.713	0.071	0.702	0.069	0.672	0.068	0.651	0.087	0.668	0.072	0.651	0.081
	0.75	0.702	0.126	0.681	0.123	0.653	0.123	0.635	0.137	0.645	0.122	0.632	0.138
BS	0	0.160	0.011	0.161	0.010	0.170	0.012	0.171	0.013	0.170	0.013	0.171	0.014
	0.25	0.132	0.015	0.134	0.015	0.138	0.015	0.140	0.015	0.138	0.015	0.139	0.016
	0.5	0.114	0.027	0.114	0.027	0.117	0.027	0.119	0.027	0.117	0.027	0.119	0.027
	0.75	0.096	0.027	0.097	0.027	0.099	0.027	0.100	0.027	0.100	0.028	0.100	0.027
$\rho = 0.1, \sigma^2 = 0.5, \alpha^* = 0.5, \gamma^* = 0.5$													
AUC	0	0.850	0.021	0.816	0.025	0.803	0.024	0.796	0.027	0.801	0.026	0.795	0.028
	0.25	0.806	0.046	0.786	0.052	0.781	0.050	0.776	0.050	0.779	0.052	0.776	0.051
	0.5	0.796	0.064	0.778	0.067	0.770	0.063	0.768	0.066	0.773	0.065	0.771	0.065
	0.75	0.811	0.099	0.802	0.099	0.794	0.101	0.798	0.100	0.793	0.104	0.798	0.102
BS	0	0.154	0.008	0.159	0.009	0.161	0.009	0.162	0.010	0.161	0.009	0.162	0.010
	0.25	0.102	0.016	0.105	0.017	0.105	0.017	0.106	0.017	0.106	0.017	0.106	0.017
	0.5	0.077	0.018	0.078	0.018	0.079	0.018	0.078	0.018	0.079	0.018	0.078	0.018
	0.75	0.052	0.015	0.053	0.016	0.054	0.016	0.054	0.016	0.054	0.016	0.054	0.016
$\rho = 0.1, \sigma^2 = 1, \alpha^* = 0.5, \gamma^* = 0.5$													
AUC	0	0.854	0.025	0.806	0.030	0.791	0.032	0.784	0.031	0.789	0.033	0.786	0.031
	0.25	0.812	0.047	0.790	0.054	0.781	0.054	0.776	0.053	0.783	0.057	0.780	0.052
	0.5	0.785	0.078	0.769	0.078	0.761	0.076	0.758	0.081	0.764	0.079	0.765	0.078
	0.75	0.811	0.108	0.791	0.104	0.779	0.109	0.771	0.110	0.777	0.116	0.779	0.109
BS	0	0.151	0.009	0.160	0.008	0.161	0.009	0.163	0.009	0.162	0.009	0.162	0.009
	0.25	0.107	0.014	0.110	0.015	0.110	0.015	0.110	0.015	0.110	0.015	0.110	0.015
	0.5	0.071	0.016	0.073	0.017	0.074	0.017	0.074	0.017	0.074	0.017	0.074	0.017
	0.75	0.054	0.015	0.055	0.015	0.056	0.015	0.056	0.015	0.055	0.015	0.056	0.015
$\rho = 0.1, \sigma^2 = 0.5, \alpha^* = 1, \gamma^* = 1$													
AUC	0	0.942	0.014	0.891	0.022	0.883	0.018	0.885	0.019	0.881	0.019	0.885	0.020
	0.25	0.880	0.045	0.846	0.049	0.844	0.050	0.847	0.048	0.843	0.045	0.847	0.046
	0.5	0.890	0.050	0.860	0.066	0.861	0.077	0.863	0.073	0.863	0.068	0.866	0.063
	0.75	0.875	0.074	0.869	0.073	0.867	0.067	0.868	0.076	0.866	0.076	0.869	0.076
BS	0	0.144	0.009	0.157	0.009	0.157	0.008	0.156	0.009	0.158	0.009	0.157	0.009
	0.25	0.064	0.011	0.067	0.013	0.068	0.012	0.068	0.012	0.068	0.011	0.068	0.012
	0.5	0.040	0.013	0.042	0.013	0.042	0.013	0.041	0.013	0.041	0.013	0.041	0.013
	0.75	0.028	0.012	0.028	0.012	0.028	0.011	0.028	0.011	0.028	0.011	0.028	0.011
$\rho = 0.1, \sigma^2 = 1, \alpha^* = 1, \gamma^* = 1$													
AUC	0	0.938	0.012	0.864	0.032	0.860	0.021	0.863	0.021	0.858	0.021	0.862	0.019
	0.25	0.889	0.030	0.843	0.041	0.847	0.033	0.849	0.032	0.842	0.031	0.849	0.030
	0.5	0.858	0.057	0.826	0.069	0.828	0.054	0.832	0.054	0.829	0.048	0.835	0.053
	0.75	0.900	0.073	0.856	0.077	0.861	0.094	0.866	0.092	0.863	0.090	0.866	0.090
BS	0	0.144	0.007	0.163	0.010	0.160	0.008	0.160	0.009	0.160	0.007	0.160	0.008
	0.25	0.063	0.012	0.069	0.013	0.068	0.012	0.067	0.012	0.068	0.012	0.067	0.012
	0.5	0.040	0.011	0.042	0.012	0.043	0.012	0.042	0.012	0.043	0.012	0.042	0.012
	0.75	0.028	0.010	0.030	0.011	0.030	0.010	0.030	0.010	0.030	0.010	0.030	0.010

### 4.3 Scenarios with different effects for two events

In this section, we delve into exploring scenarios where the markers and covariates have differential effects on the two causes of event. The simulation design was identical to section 4.1 except for the values of the regression parameters  $\alpha_l$  and  $\gamma_l$ . Throughout all simulations within this context, we set  $\sigma_k$  to 0.5 for  $k$  ranging from 1 to 10, while  $\gamma^*$  and  $\alpha^*$  are fixed at 0.5, and  $\rho$  is set to 0.1. We consider three scenarios as follows:

*Single effects on cause 1*

- $\alpha_1 = (-\alpha^*, -\alpha^*, \alpha^*, \alpha^*, 0, 0, 0, 0, 0, 0)^\top$
- $\gamma_1 = (\gamma^*, -\gamma^*, \underbrace{0, \dots, 0}_{10}, \gamma^*, -\gamma^*, \underbrace{0, \dots, 0}_{10})^\top$ .
- $\alpha_2 = (0, \dots, 0)^\top$
- $\gamma_2 = (\gamma^*, -\gamma^*, \underbrace{0, \dots, 0}_{10}, \gamma^*, -\gamma^*, \underbrace{0, \dots, 0}_{10})^\top$ .

*Single effects on both causes*

- $\alpha_1 = (\alpha^*, \alpha^*, 0, 0, 0, 0, 0, 0, 0, 0)^\top$
- $\gamma_1 = (\gamma^*, \gamma^*, \underbrace{0, \dots, 0}_{22})^\top$ .
- $\alpha_2 = (0, 0, \alpha^*, \alpha^*, 0, 0, 0, 0, 0, 0)^\top$
- $\gamma_2 = (\underbrace{0, \dots, 0}_{12}, \gamma^*, \gamma^*, \underbrace{0, \dots, 0}_{10})^\top$ .

*Opposite effects on the two causes*

- $\alpha_1 = (-\alpha^*, -\alpha^*, \alpha^*, \alpha^*, 0, 0, 0, 0, 0, 0)^\top$
- $\gamma_1 = (\gamma^*, -\gamma^*, \underbrace{0, \dots, 0}_{10}, \gamma^*, -\gamma^*, \underbrace{0, \dots, 0}_{10})^\top$ .
- $\alpha_2 = (\alpha^*, \alpha^*, -\alpha^*, -\alpha^*, 0, 0, 0, 0, 0, 0)^\top$
- $\gamma_2 = (-\gamma^*, \gamma^*, \underbrace{0, \dots, 0}_{10}, -\gamma^*, \gamma^*, \underbrace{0, \dots, 0}_{10})^\top$ .

By analyzing the findings from Table 3, which focuses on variable selection, and Table 4, which pertains to risk prediction, We observe that the differing association structures between the two events have minimal impact on the performance of the VSJM method.

**Table 3** Simulation results with differential effects between events: Mean and standard deviation of the true positive rate (TPR), false positive rate (FPR), and Matthews Correlation Coefficient (MCC) over 100 replications for  $\rho = 0.1$ ,  $\sigma^2 = 0.5$ ,  $\alpha^* = 0.5$ ,  $\gamma^* = 0.5$ . The results of DS and CS are based on a threshold of 1 for *BF* and a threshold of 0.05 for *lBFDR*.

		CS						DS					
		Total		L-Markers		Fixed covariates		Total		L-Markers		Fixed covariates	
		Est.	SD.	Est.	SD.	Est.	SD.	Est.	SD.	Est.	SD.	Est.	SD.
Single effects on cause 1													
<i>BF</i>	TPR	1.000	0.000	1.000	0.000	1.000	0.000	1.000	0.000	1.000	0.000	1.000	0.000
	FPR	0.018	0.018	0.022	0.049	0.017	0.020	0.039	0.024	0.056	0.060	0.035	0.023
	MCC	0.945	0.051	0.975	0.055	0.869	0.138	0.890	0.061	0.937	0.068	0.754	0.112
<i>lBFDR</i>	TPR	1.000	0.000	1.000	0.000	1.000	0.000	1.000	0.000	1.000	0.000	1.000	0.000
	FPR	0.000	0.000	0.000	0.000	0.000	0.000	0.002	0.006	0.000	0.000	0.003	0.008
	MCC	1.000	0.000	1.000	0.000	1.000	0.000	0.993	0.019	1.000	0.000	0.974	0.068
Single effects on both causes													
<i>BF</i>	TPR	0.963	0.060	1.000	0.000	0.925	0.121	0.975	0.053	1.000	0.000	0.950	0.105
	FPR	0.020	0.027	0.050	0.087	0.009	0.016	0.035	0.032	0.069	0.080	0.023	0.024
	MCC	0.908	0.123	0.914	0.144	0.912	0.116	0.868	0.109	0.874	0.132	0.867	0.130
<i>lBFDR</i>	TPR	0.863	0.092	1.000	0.000	0.725	0.184	0.887	0.071	1.000	0.000	0.775	0.142
	FPR	0.000	0.000	0.000	0.000	0.000	0.000	0.003	0.011	0.013	0.040	0.000	0.000
	MCC	0.919	0.055	1.000	0.000	0.836	0.115	0.922	0.060	0.976	0.075	0.869	0.086
Opposite effects on the two causes													
<i>BF</i>	TPR	0.981	0.030	1.000	0.000	0.963	0.060	0.988	0.026	1.000	0.000	0.975	0.053
	FPR	0.015	0.015	0.025	0.040	0.013	0.018	0.044	0.027	0.058	0.056	0.040	0.038
	MCC	0.956	0.044	0.971	0.047	0.943	0.066	0.908	0.049	0.933	0.063	0.887	0.093
<i>lBFDR</i>	TPR	0.850	0.053	1.000	0.000	0.700	0.105	0.881	0.069	1.000	0.000	0.762	0.138
	FPR	0.000	0.000	0.000	0.000	0.000	0.000	0.006	0.013	0.000	0.000	0.008	0.017
	MCC	0.901	0.035	1.000	0.000	0.811	0.070	0.910	0.055	1.000	0.000	0.829	0.105

**Table 4** Simulation results with differential effects between events: Mean and standard deviation of AUC and Brier score computed for landmark times  $s = 0, 0.25, 0.5, 0.75$  and prediction window of 0.25 for  $\rho = 0.1, \sigma^2 = 0.5, \alpha^* = 0.5, \gamma^* = 0.5$ .

		Real		Oracle		CS				DS			
						<i>BF</i>		<i>IBFDR</i>		<i>BF</i>		<i>IBFDR</i>	
s		Est.	SD.	Est.	SD.	Est.	SD.	Est.	SD.	Est.	SD.	Est.	SD.
Single effects on cause 1													
AUC	0	0.781	0.029	0.747	0.026	0.742	0.019	0.740	0.020	0.742	0.017	0.737	0.020
	0.25	0.790	0.047	0.759	0.060	0.761	0.050	0.762	0.053	0.757	0.052	0.757	0.053
	0.5	0.786	0.063	0.766	0.057	0.769	0.054	0.772	0.058	0.769	0.059	0.771	0.066
	0.75	0.778	0.090	0.794	0.087	0.786	0.095	0.796	0.090	0.787	0.089	0.790	0.092
BS	0	0.147	0.011	0.153	0.010	0.157	0.008	0.153	0.010	0.157	0.008	0.154	0.009
	0.25	0.117	0.014	0.121	0.017	0.121	0.016	0.120	0.017	0.121	0.016	0.121	0.017
	0.5	0.075	0.019	0.077	0.019	0.077	0.017	0.077	0.019	0.077	0.018	0.076	0.019
	0.75	0.063	0.017	0.063	0.018	0.063	0.017	0.063	0.018	0.063	0.018	0.064	0.018
Single effects on both causes													
AUC	0	0.733	0.027	0.729	0.026	0.723	0.021	0.708	0.026	0.723	0.020	0.709	0.025
	0.25	0.762	0.035	0.752	0.036	0.743	0.035	0.734	0.038	0.746	0.034	0.736	0.037
	0.5	0.756	0.073	0.743	0.082	0.736	0.079	0.725	0.071	0.733	0.079	0.736	0.077
	0.75	0.756	0.073	0.730	0.071	0.741	0.064	0.736	0.056	0.730	0.066	0.743	0.060
BS	0	0.149	0.011	0.151	0.011	0.156	0.011	0.156	0.010	0.156	0.011	0.156	0.010
	0.25	0.134	0.017	0.136	0.017	0.138	0.016	0.139	0.017	0.137	0.017	0.139	0.017
	0.5	0.124	0.017	0.124	0.018	0.127	0.018	0.128	0.017	0.128	0.018	0.126	0.017
	0.75	0.100	0.020	0.106	0.020	0.104	0.018	0.106	0.019	0.106	0.019	0.105	0.019
Opposite effects on the two causes													
AUC	0	0.784	0.021	0.791	0.027	0.765	0.027	0.757	0.026	0.761	0.029	0.758	0.030
	0.25	0.762	0.042	0.762	0.039	0.753	0.048	0.745	0.048	0.745	0.039	0.745	0.040
	0.5	0.758	0.078	0.735	0.073	0.716	0.070	0.710	0.065	0.720	0.056	0.697	0.060
	0.75	0.732	0.112	0.691	0.105	0.710	0.115	0.693	0.137	0.706	0.114	0.706	0.132
BS	0	0.138	0.011	0.137	0.011	0.146	0.012	0.149	0.011	0.147	0.012	0.149	0.012
	0.25	0.136	0.017	0.137	0.019	0.140	0.021	0.143	0.022	0.143	0.020	0.143	0.022
	0.5	0.145	0.029	0.153	0.028	0.156	0.026	0.160	0.025	0.159	0.023	0.164	0.025
	0.75	0.145	0.034	0.150	0.038	0.148	0.034	0.154	0.032	0.158	0.039	0.157	0.033

## 5 Application: 3C study

### 5.1 Data description

In this section, we analyzed a subset of the Three-City (3C) Study [34] which is a French cohort study. Participants aged 65 or older were recruited from three cities (Bordeaux, Dijon, and Montpellier) and followed for over 10 years to investigate the association between vascular factors and dementia. The data includes socio-demographic information, general health information, and cognitive test scores. The application here only included the centers of Dijon and Bordeaux, where MRI exams were conducted at years 0 and 4 for both, and additionally at year 10 for Bordeaux. Except for the MRI markers, the other longitudinal markers were measured at baseline and over the follow-up visit, including years 2, 4, 7, 10, 12, and also 14 and 17 in Bordeaux only. The diagnosis of dementia among participants followed a three-step process. Initially, cognitive assessments were conducted by neuropsychologists or investigators. Suspected cases of dementia then underwent examination by clinicians, with validation by an independent expert committee comprising neurologists and geriatricians. In addition to dementia, the exact time of death was collected and is considered a competing risk.

We considered  $N = 2133$  subjects who were dementia-free at the beginning of the study and had at least one measurement for each of the longitudinal markers. Out of these subjects, 227 were diagnosed with incident dementia, and 311 died before developing dementia. Figure 2 shows the cumulative incidence function for dementia and death in this sample.

We considered seventeen longitudinal markers: three cardio-metabolic markers (body mass index (BMI), diastolic blood pressure (DBP), and systolic blood pressure (SBP)), the total number of medications (TOTMED), depressive symptomatology measured using the Center for Epidemiologic Studies-Depression scale (CESDT, the lower the better), functional dependency assessed using the Instrumental Activities of Daily Living scale (IADL, the lower the better), four cognitive tests (the visual retention test of Benton (BENTON, number of correct responses out of 15), the Isaacs set test (ISA, total number of words given in 4 semantic categories in 15 seconds), the trail making tests A and B (TMTA and TMTB, number of correct moves per minute), the total intracranial volume (TIV), and some biomarkers of neurodegeneration, including white matter volume (WMV), gray matter volume (GMV), left hippocampal volume (LHIPP), and right hippocampal volume (RHIPP); two markers of vascular brain lesions including the volumes of white matter hyperintensities in the periventricular (Peri), and deep (Deep) white matter. Figure 3 shows individual trajectories of the longitudinal markers in the 3C study, illustrating time-dependent variables. The data were pre-transformed using splines to satisfy the normality assumption of linear mixed models [5]. The minimum, maximum, and median number of repeated measurements for SBP, DBP, CESDT, BENTON, ISA, TOTMED, and IADL are 1, 8, and 5, respectively. For BMI, TMTA, and TMTB, the minimum, maximum, and median number of repeated measurements are 1, 7, and 4, respectively. The minimum, maximum, and median number of repeated measurements for WMV, GMV, TIV, RHIPP, and LHIPP are 1, 3, and 2, respectively. For Peri and Deep (which were not measured at year 10),

there are at most two repeated measures, with a median equal to 2. In addition, the model incorporates five time-invariant explanatory variables including age at enrollment ( $\frac{\text{age}-65}{10}$ ), sex (0=male, 1=female), education level (Educ, 0=less than 10 years of schooling, 1=at least 10 years of schooling), Diabetes status at baseline (1=yes), and APOE4 allele carrier status (the main genetic susceptibility factor for Alzheimer's disease, 1=presence of APOE4).

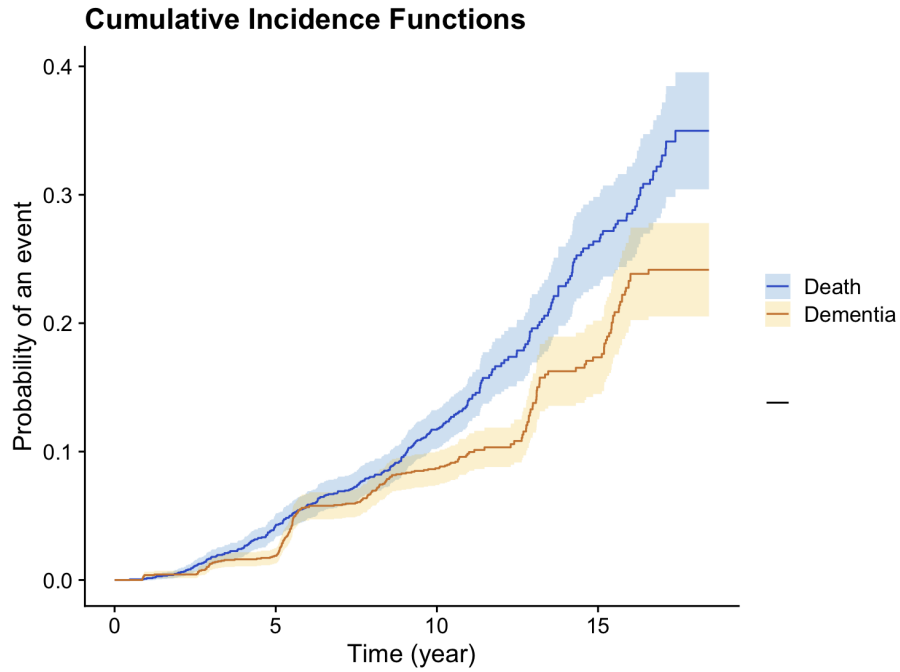
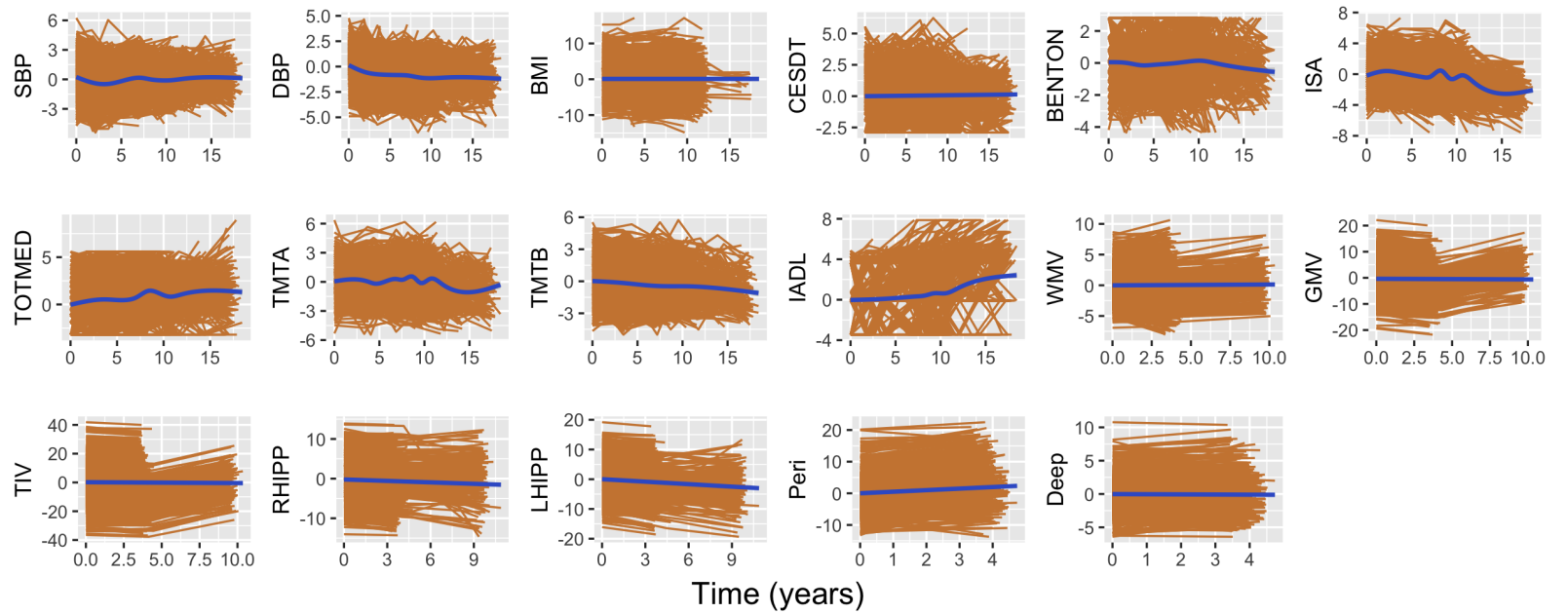


Fig. 2 Cumulative incidence function for dementia and death event over 17 years of follow-up.



**Fig. 3** Individual trajectories from the normalized clinical, neuropsychological and imaging longitudinal markers in the 3C study. Systolic blood pressure (SBP), diastolic blood pressure (DBP), body mass index (BMI), depressive symptomatology measured using the Center for Epidemiologic Studies Depression scale (CESDT), the visual retention test of Benton (BENTON), Isaacs Set Test (ISA), the total number of medications (TOTMED), the trail making test A and B (TMTA and TMTB), functional dependency assessed using Instrumental Activity of Daily Living scale (IADL), white matter volume (WMV), gray matter volume (GMV), total intracranial volume (TIV), right and left hippocampal volume (RHIPP and LHIPP), for the 5-year risk of dementia of the volumes of White Matter Hyperintensities in the periventricular (Peri) and deep (Deep) white matter.

## 5.2 Data analysis

For analyzing the 3C data using the proposed approach, we partitioned the dataset into two distinct sets: the training set, comprising 70% of the data, and a separate validation set. Parameter estimation was conducted using the training data, while risk prediction was exclusively performed on the validation set.

For this aim, a quadratic time trend is considered for both fixed and random effects, as a non-linear time trend was previously observed for SBP, DBP, BMI, CESDT, BENTON, ISA, TOTMED, TMTA, TMTB, and IADL [5]:

$$\begin{aligned} Y_{ijk} &= \eta_{ik}(s_{ijk}|\boldsymbol{\beta}_k, \mathbf{b}_{ik}) + \varepsilon_{ijk} \\ &= \beta_{0k} + \beta_{1k}s_{ijk} + \beta_{2k}s_{ijk}^2 + b_{0ik} + b_{1ik}s_{ijk} + b_{1ik}s_{ijk}^2 + \varepsilon_{ijk}. \end{aligned} \quad (22)$$

For other longitudinal markers, a linear mixed model is considered:

$$\begin{aligned} Y_{ik}(t) &= \eta_{ik}(s_{ijk}|\boldsymbol{\beta}_k, \mathbf{b}_{ik}) + \varepsilon_{ijk} \\ &= \beta_{0k} + \beta_{1k}s_{ijk} + b_{0ik} + b_{1ik}s_{ijk} + \varepsilon_{ijk}. \end{aligned} \quad (23)$$

To model dementia and death, we utilize proportional hazard models that may depend on the five time-invariant explanatory variables and the current value of the markers. Let  $\lambda_{il}(t)$  denote the cause-specific hazard function for subject  $i$ , where  $l = 1$  for dementia and  $l = 2$  for death. The proportional hazard model takes the following form:

$$\begin{aligned} \lambda_{il}(t) &= \lambda_{0l}(t) \exp(\gamma_{1l}APOE_i + \gamma_{2l}Sex_i + \gamma_{3l}Diabete_i + \gamma_{4l}Educ_i \\ &\quad + \gamma_{5l}Age_i + \sum_{k=1}^{18} \alpha_{kl}\eta_{ik}(t|\boldsymbol{\beta}_k, \mathbf{b}_{ik})). \end{aligned} \quad (24)$$

Table A.1 in the supplementary material displays the estimated regression coefficients and variance of error from the mixed effects sub-models for each marker in the one-marker joint models. Additionally, Table 5 presents the estimated parameters from the proportional hazard models for dementia and death, considering the VSJM approach given you choose DS, this is an additional reason for not emphasizing on a vague superiority of CS which is debatable in the simulation results, including estimates, standard deviations, 95% credible intervals, *lBFDRs*, and *BFs*. The analysis identifies several significant factors associated with dementia and death. Specifically, high TIV and IADL values, coupled with lower scores on the BENTON, ISA, and TMTB tests, are linked to an increased risk of dementia. Additionally, higher educational attainment, when adjusted for current cognitive scores, is also associated with a higher risk of dementia. For death without dementia, lower DBP and BENTON scores, increasing age, diabetes, and high educational levels (adjusted for current cognitive scores) are associated with a higher risk. Conversely, being female are linked to a lower risk of death. The results for CS remains similar, and are reported in Table A.2.

The predictive abilities of the model for the  $t = 5$  years prediction of dementia accounting for the competing risk of death were assessed at landmark times  $s = 0, 5$  and 10 years. To avoid overoptimistic results, AUC and BS were computed on a validation

set. The predictive abilities presented in table 6 are very good. The AUC is always higher than 0.9 except for  $s=0$  with CS and  $BF$  and higher for  $s = 5$  and 10 compared to  $s = 0$ , highlighting the information brought by the repeated measures of the longitudinal markers. Results were very similar for CS and DS priors and slightly better for  $lBFDR$  compared to  $BF$ .

**Table 5** The estimated regression coefficients and variance of errors of the longitudinal sub-model from the joint model in 3C study data using DS. Est: posterior mean, SD: standard deviation, 2.5% CI: lower bound of credible interval and 97.5% CI: upper bound of credible interval.

	Est.	SD	2.5% CI	97.5% CI	<i>lBFDR</i>	<i>BF</i>
Dementia						
WMV	0.000	0.000	0.000	0.000	1.000	0.000
GMV	0.000	0.000	0.000	0.000	1.000	0.000
TIV	0.060	0.010	0.040	0.079	0.000	Inf
RHIPP	0.000	0.000	0.000	0.000	1.000	0.000
LHIPP	-0.079	0.018	-0.115	-0.043	0.000	Inf
Peri	0.000	0.000	0.000	0.000	1.000	0.000
Deep	0.000	0.000	0.000	0.000	1.000	0.000
SBP	0.000	0.000	0.000	0.000	1.000	0.000
DBP	0.000	0.000	0.000	0.000	1.000	0.000
BMI	-0.018	0.034	-0.103	0.000	0.765	0.308
CESDT	0.013	0.043	0.000	0.171	0.900	0.111
BENTON	-0.500	0.119	-0.744	-0.272	0.000	Inf
ISA	-0.323	0.079	-0.469	-0.171	0.000	Inf
TOTMED	0.000	0.000	0.000	0.000	1.000	0.000
TMTA	0.000	0.000	0.000	0.000	1.000	0.000
TMTB	-1.140	0.110	-1.345	-0.930	0.000	Inf
IADL	0.326	0.062	0.207	0.445	0.000	Inf
Sex	0.002	0.028	0.000	0.000	0.986	0.014
Diabete	0.000	0.025	0.000	0.000	0.996	0.004
APOE	0.002	0.032	0.000	0.000	0.994	0.006
Educ	0.891	0.186	0.536	1.245	0.000	Inf
Age	0.000	0.000	0.000	0.000	1.000	0.000
Death						
WMV	0.000	0.000	0.000	0.000	1.000	0.000
GMV	0.000	0.000	0.000	0.000	1.000	0.000
TIV	0.000	0.000	0.000	0.000	1.000	0.000
RHIPP	0.000	0.000	0.000	0.000	1.000	0.000
LHIPP	0.000	0.000	0.000	0.000	1.000	0.000
Peri	0.000	0.000	0.000	0.000	1.000	0.000
Deep	0.000	0.000	0.000	0.000	1.000	0.000
SBP	0.000	0.000	0.000	0.000	1.000	0.000
DBP	-0.155	0.048	-0.248	-0.060	0.000	Inf
BMI	0.000	0.000	0.000	0.000	1.000	0.000
CESDT	0.000	0.000	0.000	0.000	1.000	0.000
BENTON	-3.347	0.132	-3.623	-3.097	0.000	Inf
ISA	0.000	0.000	0.000	0.000	1.000	0.000
TOTMED	0.000	0.000	0.000	0.000	1.000	0.000
TMTA	0.000	0.000	0.000	0.000	1.000	0.000
TMTB	0.000	0.000	0.000	0.000	1.000	0.000
IADL	0.000	0.000	0.000	0.000	1.000	0.000
Sex	-2.200	0.175	-2.553	-1.872	0.000	Inf
Diabete	1.046	0.183	0.677	1.398	0.000	Inf
APOE	0.000	0.000	0.000	0.000	1.000	0.000
Educ	0.870	0.159	0.548	1.178	0.000	Inf
Age	1.230	0.191	0.844	1.588	0.000	Inf

**Table 6** AUC and Brier score computed by validation set for landmark times  $s = 0, 5, 10$  years and prediction window of 5 years for the 3C data.

		<i>IBFDR</i>				BF			
		AUC		BS		AUC		BS	
	$s$	Est.	SD.	Est.	SD.	Est.	SD.	Est.	SD.
DS	0	0.891	0.037	0.019	0.005	0.885	0.034	0.019	0.005
	5	0.891	0.018	0.130	0.014	0.846	0.027	0.152	0.016
	10	0.971	0.016	0.044	0.016	0.901	0.035	0.122	0.029
CS	0	0.731	0.070	0.058	0.006	0.827	0.075	0.020	0.004
	5	0.851	0.022	0.184	0.016	0.895	0.017	0.109	0.012
	10	0.863	0.045	0.135	0.028	0.945	0.023	0.086	0.022

## 6 Conclusion

In this paper, we introduce a novel Bayesian approach for variable selection in joint modeling of multiple longitudinal markers and competing risks outcomes. Our method employs spike-and-slab priors for both the association parameters and the regression coefficients in the survival model. The approach involves two main steps: first, a simple Bayesian joint model is fitted separately for each longitudinal marker and competing risks outcome; second, variable selection is performed using a time-dependent Bayesian proportional hazards model, incorporating Dirac spike or continuous spike priors for the regression coefficients, including those for time-dependent markers and fixed covariates. We also propose two decision criteria, Bayes factor and local Bayesian false discovery rate (*IBFDR*), for selecting relevant variables.

A key advantage of our Bayesian variable selection approach is that the posterior distributions of the selected variables naturally account for both the uncertainty of selection and parameter estimation, without requiring re-estimation of the model using only the selected variables. This property is in contrast to frequentist post-selection approaches, where ignoring the selection uncertainty can lead to underestimated standard errors [46–48]. Consequently, the standard deviations obtained from our approach provide valid measures of uncertainty for both selection and estimation, even in the presence of multiple imputed datasets or informative dropout.

In addition to variable selection, we illustrate how our approach can be used for dynamic prediction based on the estimated joint model. We demonstrate the performance of the method via extensive simulation studies, evaluating both variable selection accuracy and predictive ability. Furthermore, we apply our method to predict dementia risk using the 3C dataset, showcasing its practical relevance. The method is implemented in the freely available R package *VSJM* (<https://github.com/tbaghfalaki/VSJM>).

Future extensions of this work could include accommodating non-Gaussian longitudinal markers by using generalized linear mixed models in the one-marker joint models. Additionally, the methodology could be expanded to perform group-wise selection, providing further flexibility for high-dimensional longitudinal data. Overall, our approach offers a computationally efficient and statistically principled framework for variable

selection and dynamic prediction in joint modeling of longitudinal and time-to-event data.

## Acknowledgements

This work was partly funded by the French National Research Agency (grant ANR-21-CE36 for the project “Joint Models for Epidemiology and Clinical research”). This study received financial support from the French government in the framework of the University of Bordeaux’s IdEx “Investments for the Future” program / RRI PHDS. The 3C Study was supported by Sanofi-Synthélabo, the FRM, the CNAM-TS, DGS, Conseils Régionaux of Aquitaine, 395 Languedoc-Roussillon, and Bourgogne; Foundation of France; Ministry of Research- INSERM “Cohorts and biological data collections” program; MGEN; Longevity Institute; General Council of the Côte d’Or; ANR PNRA 2006 (grant ANR/ DEDD/ PNRA/ PROJ/ 200206–01-01) and Longvie 2007 (grant LVIE-003-01); Alzheimer Plan Foundation (FCS grant 2009-2012); and Roche. The Three City Study data are available upon request at [e3c.coordinatingcenter@gmail.com](mailto:e3c.coordinatingcenter@gmail.com).

## References

- [1] Guedj, J., Thiébaud, R., Commenges, D.: Joint modeling of the clinical progression and of the biomarkers’ dynamics using a mechanistic model. *Biometrics* **67**(1), 59–66 (2011)
- [2] Hossain, M.A.: Multivariate joint models and dynamic predictions. PhD thesis, University of South Carolina (2020)
- [3] Shen, F., Li, L.: Backward joint model and dynamic prediction of survival with multivariate longitudinal data. *Statistics in medicine* **40**(20), 4395–4409 (2021)
- [4] Lin, J., Luo, S.: Deep learning for the dynamic prediction of multivariate longitudinal and survival data. *Statistics in medicine* **41**(15), 2894–2907 (2022)
- [5] Devaux, A., Helmer, C., Dufouil, C., Genuer, R., Proust-Lima, C.: Random survival forests for competing risks with multivariate longitudinal endogenous covariates. arXiv preprint arXiv:2208.05801 (2022)
- [6] Zhang, T., Tang, X., Zhang, Y., Xu, L., Wei, Y., Hu, Y., Cui, H., Tang, Y., Liu, H., Chen, T., *et al.*: Multivariate joint models for the dynamic prediction of psychosis in individuals with clinical high risk. *Asian Journal of Psychiatry* **81**, 103468 (2023)
- [7] Rizopoulos, D.: Dynamic predictions and prospective accuracy in joint models for longitudinal and time-to-event data. *Biometrics* **67**(3), 819–829 (2011)
- [8] Rizopoulos, D.: *Joint Models for Longitudinal and Time-to-event Data: With Applications in R*. CRC press, New York (2012)

- [9] Sousa, I.: A review on joint modelling of longitudinal measurements and time-to-event. *REVSTAT-Statistical Journal* **9**(1), 57–81 (2011)
- [10] Papageorgiou, G., Mauff, K., Tomer, A., Rizopoulos, D.: An overview of joint modeling of time-to-event and longitudinal outcomes. *Annual review of statistics and its application* **6**, 223–240 (2019)
- [11] Alsefri, M., Sudell, M., García-Fiñana, M., Kolamunnage-Dona, R.: Bayesian joint modelling of longitudinal and time to event data: a methodological review. *BMC medical research methodology* **20**, 1–17 (2020)
- [12] Zhudenkov, K., Gavrilov, S., Sofronova, A., Stepanov, O., Kudryashova, N., Helminger, G., Peskov, K.: A workflow for the joint modeling of longitudinal and event data in the development of therapeutics: Tools, statistical methods, and diagnostics. *CPT: Pharmacometrics & Systems Pharmacology* **11**(4), 425–437 (2022)
- [13] Rizopoulos, D.: The r package jmbayes for fitting joint models for longitudinal and time-to-event data using mcmc. *Journal of Statistical Software* **72**, 1–46 (2016)
- [14] Rizopoulos, D., Papageorgiou, G., Miranda Afonso, P.: Jmbayes2: extended joint models for longitudinal and time-to-event data. R package version 0.2-4 (2022)
- [15] Rustand, D., Krainski, E.T., Rue, H.: Denirustand/inlajoint: Joint modeling multivariate longitudinal and time-to-event outcomes with inla (2022)
- [16] Brilleman, S.: Estimating joint models for longitudinal and time-to-event data with rstanarm (2023)
- [17] Baghfalaki, T., Hashemi, R., Helmer, C., Jacqmin-Gadda, H.: A two-stage joint modeling approach for multiple longitudinal markers and time-to-event data. *Statistical Methods in Medical Research*, 10.1177/09622802251406588, 1–33 (2025)
- [18] Chowdhury, M.Z.I., Turin, T.C.: Variable selection strategies and its importance in clinical prediction modelling. *Family medicine and community health* **8**(1) (2020)
- [19] Bühlmann, P., Van De Geer, S.: *Statistics for High-dimensional Data: Methods, Theory and Applications*. Springer, Germany (2011)
- [20] Gelman, A., Carlin, J.B., Stern, H.S., Rubin, D.B.: *Bayesian Data Analysis*. Chapman and Hall/CRC, United States (1995)
- [21] George, E.I., McCulloch, R.E.: Variable selection via gibbs sampling. *Journal of the American Statistical Association* **88**(423), 881–889 (1993)
- [22] Malsiner-Walli, G., Wagner, H.: Comparing spike and slab priors for bayesian

- variable selection. *Austrian Journal of Statistics* **40**(4), 241–264 (2011)
- [23] Mitchell, T.J., Beauchamp, J.J.: Bayesian variable selection in linear regression. *Journal of the American Statistical Association* **83**(404), 1023–1032 (1988)
- [24] Carvalho, C.M., Polson, N.G., Scott, J.G.: The horseshoe estimator for sparse signals. *Biometrika* **97**(2), 465–480 (2010)
- [25] Williams, P.M.: Bayesian regularization and pruning using a Laplace prior. *Neural Computation* **7**(1), 117–143 (1995)
- [26] Scott, J.G., Berger, J.O.: Bayes and empirical-bayes multiplicity adjustment in the variable-selection problem. *The Annals of Statistics*, 2587–2619 (2010)
- [27] He, Z., Tu, W., Wang, S., Fu, H., Yu, Z.: Simultaneous variable selection for joint models of longitudinal and survival outcomes. *Biometrics* **71**(1), 178–187 (2015)
- [28] Yi, F., Tang, N., Sun, J.: Simultaneous variable selection and estimation for joint models of longitudinal and failure time data with interval censoring. *Biometrics* **78**(1), 151–164 (2022)
- [29] Griesbach, C., Mayr, A., Bergherr, E.: Variable selection and allocation in joint models via gradient boosting techniques. *Mathematics* **11**(2), 411 (2023)
- [30] Chen, Y., Wang, Y.: Variable selection for joint models of multivariate longitudinal measurements and event time data. *Statistics in Medicine* **36**(24), 3820–3829 (2017)
- [31] Tang, J., Tang, A.-M., Tang, N.: Variable selection for joint models of multivariate skew-normal longitudinal and survival data. *Statistical Methods in Medical Research* **32**(9), 1694–1710 (2023)
- [32] Xie, Y., He, Z., Tu, W., Yu, Z.: Variable selection for joint models with time-varying coefficients. *Statistical Methods in Medical Research* **29**(1), 309–322 (2020)
- [33] Tang, A.-M., Zhao, X., Tang, N.-S.: Bayesian variable selection and estimation in semiparametric joint models of multivariate longitudinal and survival data. *Biometrical Journal* **59**(1), 57–78 (2017)
- [34] Antoniak, M., Pugliatti, M., Hubbard, R., Britton, J., Sotgiu, S., Sadovnick, A.D., Yee, I.M., Cumsille, M.A., Bevilacqua, J.A., Burdett, S., *et al.*: Vascular factors and risk of dementia: design of the three-city study and baseline characteristics of the study population. *Neuroepidemiology* **22**(6), 316–325 (2003)
- [35] Ibrahim, J.G., Chen, M.-H., Sinha, D., Ibrahim, J., Chen, M.: *Bayesian Survival Analysis* vol. 2. Springer, Germany (2001)

- [36] He, P., Kong, G., Su, Z.: Estimating the survival functions for right-censored and interval-censored data with piecewise constant hazard functions. *Contemporary clinical trials* **35**(2), 122–127 (2013)
- [37] Chi, Y.-Y., Ibrahim, J.G.: Joint models for multivariate longitudinal and multivariate survival data. *Biometrics* **62**(2), 432–445 (2006)
- [38] Song, X., Davidian, M., Tsiatis, A.A.: An estimator for the proportional hazards model with multiple longitudinal covariates measured with error. *Biostatistics* **3**(4), 511–528 (2002)
- [39] Xu, J., Zeger, S.L.: The evaluation of multiple surrogate endpoints. *Biometrics* **57**(1), 81–87 (2001)
- [40] Rizopoulos, D., Ghosh, P.: A bayesian semiparametric multivariate joint model for multiple longitudinal outcomes and a time-to-event. *Statistics in medicine* **30**(12), 1366–1380 (2011)
- [41] Baghfalaki, T., Ganjali, M., Berridge, D.: Joint modeling of multivariate longitudinal mixed measurements and time to event data using a bayesian approach. *Journal of Applied Statistics* **41**(9), 1934–1955 (2014)
- [42] Long, J.D., Mills, J.A.: Joint modeling of multivariate longitudinal data and survival data in several observational studies of huntington’s disease. *BMC medical research methodology* **18**(1), 1–15 (2018)
- [43] Baghfalaki, T., Ganjali, M.: Approximate bayesian inference for joint linear and partially linear modeling of longitudinal zero-inflated count and time to event data. *Statistical Methods in Medical Research* **30**(6), 1484–1501 (2021)
- [44] Bogaert, I.: Iteration-free computation of gauss–legendre quadrature nodes and weights. *SIAM Journal on Scientific Computing* **36**(3), 1008–1026 (2014)
- [45] Tanton, J.: *Encyclopedia of Mathematics*. Facts On File, Inc, United States (2005)
- [46] George, E.I., McCulloch, R.E.: Variable selection via gibbs sampling. *Journal of the American Statistical Association* **88**(423), 881–889 (1993)
- [47] O’Hara, R.B., Sillanpää, M.J.: A review of bayesian variable selection methods: what, how and which. *Bayesian Analysis* **4**(1), 85–117 (2009)
- [48] Malsiner-Walli, G., Frühwirth-Schnatter, S., Wagner, H.: Comparing spike-and-slab priors for bayesian variable selection. *Bayesian Analysis* **13**(1), 223–248 (2018)
- [49] Xu, X., Ghosh, M., *et al.*: Bayesian variable selection and estimation for group lasso. *Bayesian Analysis* **10**(4), 909–936 (2015)

- [50] Plummer, M., *et al.*: Jags: A program for analysis of bayesian graphical models using gibbs sampling. In: Proceedings of the 3rd International Workshop on Distributed Statistical Computing, vol. 124, pp. 1–10 (2003). Vienna, Austria
- [51] Plummer, M.: Jags version 3.3. 0 user manual. International Agency for Research on Cancer, Lyon, France (2012)
- [52] Su, Y.-S., Yajima, M.: R2jags: Using r to run ‘jags’. R package version 0.5-7 **34** (2015)
- [53] Efron, B.: Large-scale Inference: Empirical Bayes Methods for Estimation, Testing, and Prediction vol. 1. Cambridge University Press, United Kingdom (2012)
- [54] Kass, R.E., Raftery, A.E.: Bayes factors. Journal of the american statistical association **90**(430), 773–795 (1995)
- [55] Benjamini, Y., Hochberg, Y.: Controlling the false discovery rate: a practical and powerful approach to multiple testing. Journal of the Royal statistical society: series B (Methodological) **57**(1), 289–300 (1995)
- [56] Efron, B., Gous, A., Kass, R., Datta, G., Lahiri, P.: Scales of evidence for model selection: Fisher versus jeffreys. Lecture Notes-Monograph Series, 208–256 (2001)
- [57] Efron, B., Tibshirani, R.: Empirical bayes methods and false discovery rates for microarrays. Genetic epidemiology **23**(1), 70–86 (2002)
- [58] Efron, B.: Large-scale simultaneous hypothesis testing: the choice of a null hypothesis. Journal of the American Statistical Association **99**(465), 96–104 (2004)
- [59] Sampson, J.N., Chatterjee, N., Carroll, R.J., Müller, S.: Controlling the local false discovery rate in the adaptive lasso. Biostatistics **14**(4), 653–666 (2013)
- [60] Yap, J.K., Gauran, I.I.M.: Bayesian variable selection using knockoffs with applications to genomics. Computational Statistics **38**(4), 1771–1790 (2023)
- [61] Majumdar, A., Haldar, T., Bhattacharya, S., Witte, J.S.: An efficient bayesian meta-analysis approach for studying cross-phenotype genetic associations. PLoS genetics **14**(2), 1007139 (2018)
- [62] Baghfalaki, T., Sugier, P.-E., Truong, T., Pettitt, A.N., Mengersen, K., Lique, B.: Bayesian meta-analysis models for cross cancer genomic investigation of pleiotropic effects using group structure. Statistics in Medicine **40**(6), 1498–1518 (2021)
- [63] Zhou, X., Reiter, J.P.: A note on bayesian inference after multiple imputation. The American Statistician **64**(2), 159–163 (2010)

- [64] Steyerberg, E.W.: Applications of prediction models. In: *Clinical Prediction Models*, pp. 11–31. Springer, Germany (2009)
- [65] Blanche, P., Proust-Lima, C., Loubère, L., Berr, C., Dartigues, J.-F., Jacqmin-Gadda, H.: Quantifying and comparing dynamic predictive accuracy of joint models for longitudinal marker and time-to-event in presence of censoring and competing risks. *Biometrics* **71**(1), 102–113 (2015)
- [66] Matthews, B.W.: Comparison of the predicted and observed secondary structure of t4 phage lysozyme. *Biochimica et Biophysica Acta (BBA) - Protein Structure* **405**(2), 442–451 (1975) [https://doi.org/10.1016/0005-2795\(75\)90109-9](https://doi.org/10.1016/0005-2795(75)90109-9)
- [67] Austin, P.C.: Generating survival times to simulate cox proportional hazards models with time-varying covariates. *Statistics in medicine* **31**(29), 3946–3958 (2012)
- [68] Ross, S.M.: *Simulation*, 5th Edision. Academic Press, October (2012)

## Supplementary Material

**Table A.1** Estimated regression coefficients and error variances from the longitudinal sub-model in the 3C study. Est.: posterior mean; SD: standard deviation; 2.5% CI: lower bound of credible bound; 97.5% CI: upper bound of credible bound.

		Est.	SD	2.5% CI	97.5% CI
WMV	Intercept	-0.004	0.063	-0.119	0.114
	Time	0.027	0.012	0.004	0.051
	$\sigma^2$	0.765	0.063	0.629	0.875
GMV	Intercept	-0.102	0.145	-0.382	0.170
	Time	-0.246	0.021	-0.285	-0.205
	$\sigma^2$	1.994	0.107	1.797	2.216
TIV	Intercept	-0.293	0.299	-0.779	0.420
	Time	0.019	0.028	-0.037	0.074
	$\sigma^2$	3.760	0.199	3.394	4.168
RHIPP	Intercept	0.137	0.100	-0.042	0.327
	Time	-0.316	0.013	-0.340	-0.291
	$\sigma^2$	0.905	0.054	0.801	1.018
LHIPP	Intercept	0.087	0.112	-0.128	0.297
	Time	-0.350	0.014	-0.379	-0.322
	$\sigma^2$	1.017	0.062	0.900	1.144
Peri	Intercept	-0.074	0.116	-0.310	0.132
	Time	0.605	0.029	0.549	0.661
	$\sigma^2$	1.704	0.493	0.945	2.671
Deep	Intercept	-0.009	0.058	-0.120	0.108
	Time	0.019	0.012	-0.004	0.043
	$\sigma^2$	0.601	0.097	0.394	0.770
SBP	Intercept	0.053	0.085	-0.071	0.198
	Time	-0.327	0.286	-0.668	-0.027
	Time <sup>2</sup>	0.064	0.071	-0.008	0.140
	$\sigma^2$	0.994	0.037	0.934	1.072
DBP	Intercept	-0.038	0.108	-0.179	0.118
	Time	-0.488	0.339	-0.863	-0.135
	Time <sup>2</sup>	0.075	0.084	-0.010	0.162
	$\sigma^2$	0.967	0.040	0.907	1.062
BMI	Intercept	0.014	0.225	-0.273	0.299
	Time	0.015	0.047	-0.057	0.079
	Time <sup>2</sup>	0.003	0.017	-0.015	0.022
	$\sigma^2$	0.997	0.044	0.933	1.100
CESDT	Intercept	0.053	0.163	-0.160	0.258
	Time	-0.060	0.196	-0.305	0.150
	Time <sup>2</sup>	0.011	0.054	-0.044	0.070
	$\sigma^2$	1.029	0.028	0.981	1.091
BENTON	Intercept	0.110	0.063	0.010	0.235
	Time	-0.239	0.223	-0.517	0.000
	Time <sup>2</sup>	0.049	0.053	-0.005	0.107
	$\sigma^2$	0.980	0.030	0.925	1.037
ISA	Intercept	0.069	0.113	-0.079	0.251
	Time	-0.143	0.229	-0.436	0.109
	Time <sup>2</sup>	0.029	0.051	-0.023	0.085
	$\sigma^2$	0.963	0.027	0.911	1.017
TOTMED	Intercept	-0.096	0.118	-0.264	0.061
	Time	-0.038	0.327	-0.426	0.304
	Time <sup>2</sup>	0.038	0.077	-0.041	0.121
	$\sigma^2$	1.053	0.046	0.977	1.140
TMTA	Intercept	0.044	0.033	-0.021	0.104
	Time	-0.193	0.245	-0.500	0.067
	Time <sup>2</sup>	0.051	0.057	-0.007	0.113
	$\sigma^2$	0.957	0.049	0.879	1.058
TMTB	Intercept	-0.000	0.035	-0.068	0.069
	Time	-0.250	0.205	-0.492	-0.031
	Time <sup>2</sup>	0.040	0.054	-0.015	0.098
	$\sigma^2$	0.975	0.052	0.893	1.091
IADL	Intercept	0.015	0.123	-0.144	0.180
	Time	-0.055	0.089	-0.175	0.050
	Time <sup>2</sup>	0.020	0.025	-0.006	0.048
	$\sigma^2$	0.969	0.032	0.915	1.038

**Table A.2** The estimated regression coefficients and variance of errors of the longitudinal sub-model from the joint model in 3C study data using CS. Est: posterior mean, SD: standard deviation, 2.5% CI: lower bound of credible interval and 97.5% CI: upper bound of credible interval.

	Est.	SD	2.5% CI	97.5% CI	<i>lBFDR</i>	BF
Dementia						
WMV	-0.030	0.022	-0.076	0.008	0.991	0.009
GMV	0.009	0.019	-0.029	0.042	1.000	0.000
TIV	0.033	0.011	0.011	0.053	1.000	0.000
RHIPP	-0.020	0.019	-0.055	0.015	1.000	0.000
LHIPP	-0.042	0.021	-0.085	-0.001	1.000	0.000
Peri	0.021	0.015	-0.005	0.053	1.000	0.000
Deep	0.020	0.026	-0.037	0.065	1.000	0.000
SBP	-0.006	0.040	-0.078	0.062	0.988	0.012
DBP	-0.041	0.032	-0.102	0.020	1.000	0.000
BMI	-0.003	0.014	-0.032	0.027	1.000	0.000
CESDT	0.038	0.030	-0.022	0.100	1.000	0.000
BENTON	-0.893	0.187	-1.251	-0.604	0.000	Inf
ISA	-0.034	0.031	-0.094	0.027	1.000	0.000
TOTMED	-0.040	0.033	-0.107	0.019	1.000	0.000
TMTA	0.004	0.042	-0.077	0.074	1.000	0.000
TMTB	-0.851	0.489	-1.344	-0.079	0.297	2.364
IADL	0.440	0.089	0.296	0.623	0.000	Inf
Sex	-0.001	0.032	-0.062	0.061	1.000	0.000
Diabete	0.009	0.054	-0.054	0.071	0.979	0.021
APOE	0.688	0.183	0.311	1.020	0.000	Inf
Educ	0.641	0.175	0.283	0.951	0.000	Inf
Age	0.005	0.049	-0.063	0.082	0.955	0.047
Death						
WMV	0.016	0.023	-0.030	0.061	1.000	0.000
GMV	-0.010	0.019	-0.046	0.026	1.000	0.000
TIV	0.029	0.011	0.008	0.051	1.000	0.000
RHIPP	-0.007	0.017	-0.038	0.024	1.000	0.000
LHIPP	0.018	0.018	-0.015	0.052	1.000	0.000
Peri	0.001	0.011	-0.020	0.023	1.000	0.000
Deep	0.002	0.025	-0.045	0.053	1.000	0.000
SBP	0.004	0.028	-0.051	0.057	1.000	0.000
DBP	0.296	0.047	0.203	0.393	0.000	Inf
BMI	0.012	0.010	-0.008	0.031	1.000	0.000
CESDT	-0.003	0.025	-0.050	0.050	1.000	0.000
BENTON	-0.088	0.030	-0.152	-0.032	1.000	0.000
ISA	-1.761	0.084	-1.936	-1.620	0.000	Inf
TOTMED	0.075	0.027	0.022	0.129	1.000	0.000
TMTA	0.014	0.028	-0.041	0.064	1.000	0.000
TMTB	0.014	0.027	-0.041	0.068	1.000	0.000
IADL	0.011	0.025	-0.040	0.058	1.000	0.000
Sex	-1.816	0.196	-2.088	-1.813	0.000	Inf
Diabete	0.125	0.221	-0.050	0.662	0.763	0.311
APOE	0.002	0.039	-0.063	0.067	0.979	0.021
Educ	0.001	0.032	-0.062	0.067	1.000	0.000
Age	1.227	0.170	0.864	1.543	0.000	Inf